USGS
science for a changing world

Prepared in cooperation with Clean Water Services

Modeling Hydrodynamics, Temperature, and Water Quality in Henry Hagg Lake, Oregon, 2000–03

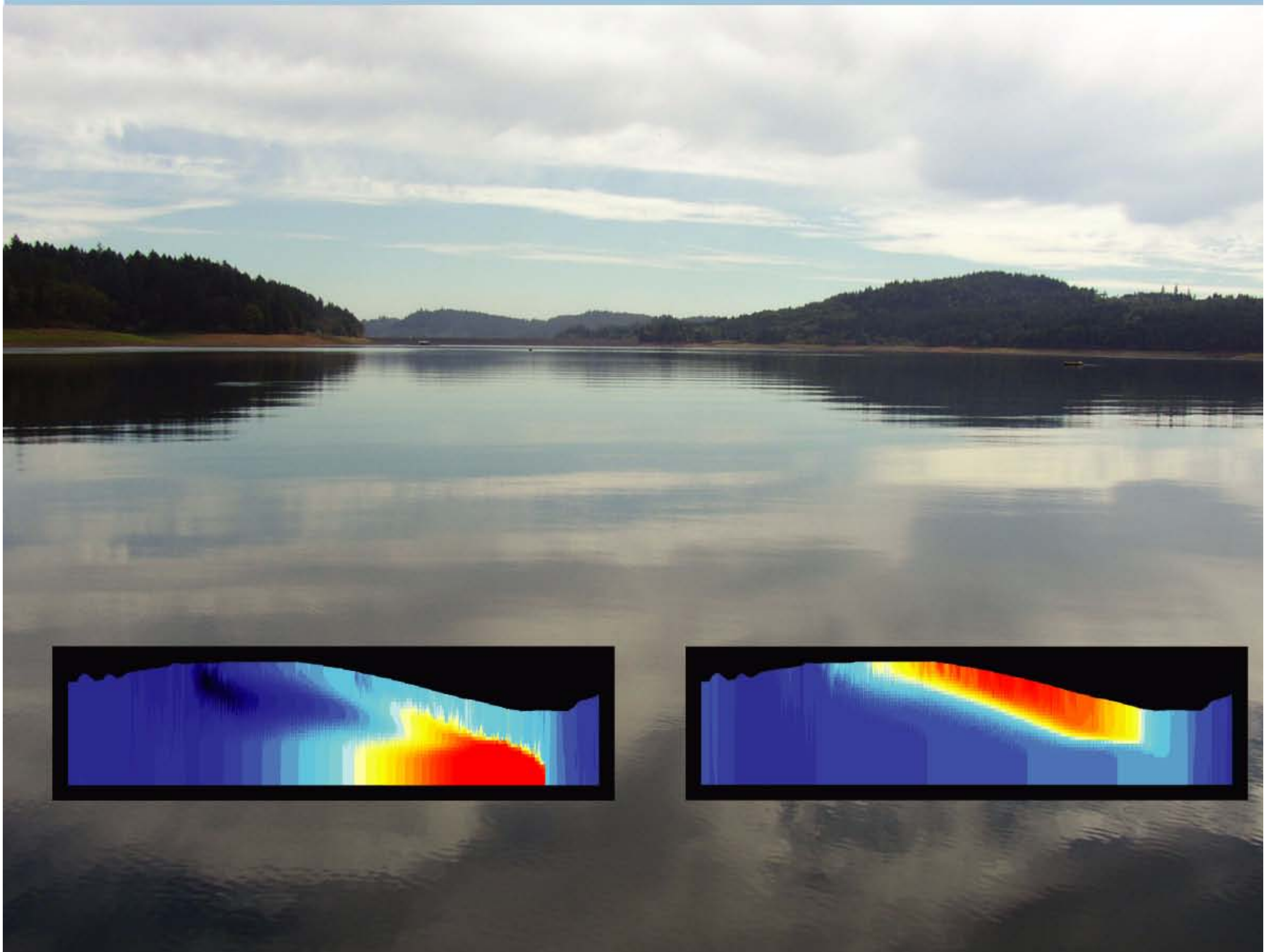

Scientific Investigations Report 2004–5261

U.S. Department of the Interior
U.S. Geological Survey

Front Cover:

Henry Hagg Lake looking toward Scoggins Dam, taken on Sept. 22, 2004. *Photograph by Stewart Rounds (U.S. Geological Survey).*

Modeling Hydrodynamics, Temperature, and Water Quality in Henry Hagg Lake, Oregon, 2000–03

By Annett B. Sullivan and Stewart A. Rounds

Prepared in cooperation with Clean Water Services

Scientific Investigations Report 2004–5261

U.S. Department of the Interior
U.S. Geological Survey

U.S. Department of the Interior
Gale A. Norton, Secretary

U.S. Geological Survey
Charles G. Groat, Director

U.S. Geological Survey, Portland, Oregon: 2005

For sale by U.S. Geological Survey, Information Services
Box 25286, Denver Federal Center
Denver, CO 80225

For more information about the USGS and its products:
Telephone: 1-888-ASK-USGS
World Wide Web: http://www.usgs.gov/

Calibrated models for 2000–03, as well as visualizations of model output, as used in this study, are available from the Internet at http://or.water.usgs.gov/tualatin/hagg_lake/.

Suggested citation:
Sullivan, A.B., and Rounds, S.A., 2005, Modeling hydrodynamics, temperature, and water quality in Henry Hagg Lake, Oregon, 2000–03: U.S. Geological Survey Scientific Investigations Report 2004–5261, 38 p.

CONTENTS

Figures

Tables

Conversion Factors

Multiply	By	To obtain
gram (g)	0.03527	ounce, avoirdupois (oz)
liter (L)	33.82	ounce, fluid (fl. oz)
meter (m)	3.281	foot (ft)
square meter (m^2)	10.76	square foot (ft^2)
cubic meter (m^3)	35.31	cubic foot (ft^3)
cubic meter (m^3)	0.0008107	acre-foot

Temperature in degrees Celsius (°C) may be converted to degrees Fahrenheit (°F) as follows:

$$°F = (1.8 \times °C) + 32$$

Vertical coordinate information is referenced to the National Geodetic Vertical Datum of 1929 (NGVD29).

Horizontal coordinate information is referenced to the North American Datum of 1983 (NAD83).

Base map compiled from various digital geospatial datasets. The projection is Lambert Conformal Conic, NAD83, units 3.28084 with parallels at 43°00′00″ and 43°30′00″, central meridian 120°30′00″ W and base parallel at 41°45′00″.

This page left intentionally blank

Modeling Hydrodynamics, Temperature, and Water Quality in Henry Hagg Lake, Oregon, 2000–03

By Annett B. Sullivan and Stewart A. Rounds

Abstract

The two-dimensional model CE-QUAL-W2 was used to simulate hydrodynamics, temperature, and water quality in Henry Hagg Lake, Oregon, for the years 2000 through 2003. Input data included lake bathymetry, meteorologic conditions, tributary inflows, tributary temperature and water quality, and lake outflows. Calibrated constituents included lake hydrodynamics, water temperature, orthophosphate, total phosphorus, ammonia, algae, chlorophyll *a*, zooplankton, and dissolved oxygen. Other simulated constituents included nitrate, dissolved and particulate organic matter, dissolved solids, and suspended sediment. Two algal groups (blue-green algae, and all other algae) were included in the model to simulate the lake's algal communities. Measured lake stage data were used to calibrate the lake's water balance; calibration of water temperature and water quality relied upon vertical profile data taken in the deepest part of the lake near the dam. The model initially was calibrated with data from 2000–01 and tested with data from 2002–03. Sensitivity tests were performed to examine the response of the model to specific parameters and coefficients, including the light-extinction coefficient, wind speed, tributary inflows of phosphorus, nitrogen and organic matter, sediment oxygen demand, algal growth rates, and zooplankton feeding preference factors.

Significant findings from this study include:

1. Lake levels were highest in late spring and early summer and decreased through the summer and fall as downstream users required water for irrigation, drinking water, flow augmentation, and municipal uses. Lake levels were lowest in November and began to rise with the onset of winter rains. A drought during the winter of 2000–01 caused the reservoir to not fill in 2001. The annual cycle in lake level was an important factor that affected lake temperature and water quality.
2. Spatial and temporal patterns in water temperature in Henry Hagg Lake were similar in all 4 years modeled in this study. A thermocline developed each year by early summer, isolating cold, dense water near the bottom, below the lake's outlet structure. Withdrawals from the lake, as well as other seasonal factors, tended to draw the thermocline down to the level of the lake's outlet structure by mid-summer. Henry Hagg Lake typically turned over in November and remained uniformly mixed and isothermal until early March, when temperature stratification began. Meteorological factors (solar energy, air temperature, wind) and reservoir operations (lake stage, elevation of the withdrawal) were found to have significant influences on the lake's water temperature.
3. During normal years, dissolved oxygen became depleted in the hypolimnion by late September; during the drought year, this occurred earlier, by late August. Colder temperatures and lake turnover in November reoxygenated the water column and ended hypolimnetic anoxia in each year. Dissolved oxygen levels in Henry Hagg Lake were controlled mainly by water temperature (solubility), sediment oxygen demand, and, to a lesser degree, by algal photosynthesis and respiration.
4. Ammonia concentrations generally were low throughout Henry Hagg Lake. However, in all years studied, accumulation of ammonia in the hypolimnion occurred once dissolved oxygen was depleted. Ammonia concentrations as high as 0.43 mg/L (milligrams per liter) as N were measured in November of 2000.
5. Algae were separated into two groups in the model: blue-green algae and all other algae. The general algae group had its highest abundance in the spring, due in part to inputs of algae from tributaries and possible resuspension of algal cells during storms. The blue-green algae group tended to bloom in late summer (in August, typically). Orthophosphate concentrations, as well as zooplankton grazing, water temperature, and light, controlled the levels and timing of algal blooms in the model. Concentrations of bioavailable phosphorus appeared to limit the size of the annual blue-green algae bloom.
6. While a community of zooplankton was found in Henry Hagg Lake, its interactions with other zooplankton and with the lake's algal communities appears to be significantly more complex than what was represented in the model. Future work may be required to better describe

the influence of zooplankton on the lake's water quality.

7. The model captured the dominant processes affecting water quality (temperature, dissolved oxygen, nutrients, and algae) in Henry Hagg Lake and simulated the lake's water-quality dynamics with sufficient accuracy for the planned purposes of the model. Comparing measured and modeled water temperature profiles for the 4 years simulated, the mean absolute error (MAE) was less than 0.7°C and the root mean square error (RMSE) was less than 1°C. Comparing measured and modeled dissolved oxygen profiles in the 3 years having reliable data (2000–02), the model errors typically were less than 1 mg/L.

Introduction

Henry Hagg Lake is a reservoir located in the foothills of the eastern slope of the Coast Range Mountains of northwestern Oregon (fig. 1), approximately 5 miles southwest of the city of Forest Grove and 25 miles west of the city of Portland. The lake was formed by Scoggins Dam, an earthfill structure that impounds Scoggins Creek, a tributary of the Tualatin River, which flows into the Willamette River. Sain Creek and Tanner Creek also drain directly into Henry Hagg Lake, and the total drainage area upstream of the dam is 40.6 square miles. Henry Hagg Lake was filled and began normal operation in 1975. At a maximum water elevation of 93.2 m (meters) (305.8 feet [ft]) above sea level (NGVD29) (Ferrari, 2001), the lake's total storage capacity is 64,812 acre-feet, with a maximum surface area of 1.8 square miles. The normal full pool water elevation is 92.5 m (303.5 ft), with a capacity of 62,216 acre-feet and a surface area of 1.7 square miles. The dam was built and is owned by the Bureau of Reclamation, which contracts with the Tualatin Valley Irrigation District (TVID) for operation and maintenance.

The Henry Hagg Lake area is characterized by warm, dry summers and cool, wet winters. From 1971–2000, the mean annual temperature in Forest Grove was 11.7°C (degrees Celsius) (Taylor, 2002). The coldest monthly mean temperature generally occurs in January (3.9°C), while the warmest month is usually August (20.4°C). The mean annual precipitation is 117 centimeters (cm), and almost 75% falls between November and March.

The Scoggins Creek valley is underlain by recent (Holocene) stream alluvium, and clay and silt soils. Bedrock in the area consists of Tertiary marine volcanic and sedimentary formations (Schlicker and Deacon, 1967). These formations dip gently in an east to northeast direction. Western hemlock and Douglas fir cover approximately 82% of the watershed; mountain snowberry and mountain sagebrush cover approximately 5% (Estrada, 2000).

The lake is used for recreation in the summer and flood control in the winter. It provides irrigation water to agricultural areas of the basin and municipal and industrial water to the cities of Forest Grove, Cornelius, Hillsboro, Beaverton, and several smaller towns. Water from Henry Hagg Lake also is used by Clean Water Services (CWS), the primary water-management agency in the Tualatin River Basin, to augment flow in the lower Tualatin River in order to enhance water quality and help the river meet water-quality standards.

Municipal and industrial demand for water in the Tualatin Basin is projected to almost double by 2050 due to population growth (Montgomery Watson Harza, 2004). Several options are being considered to meet this expected demand, including structural changes to Scoggins Dam. Modifications under consideration include raising Scoggins Dam by 6.1 or 12.2 m (20 or 40 ft) and installing a pipeline from the reservoir directly to a major user. Any dam raise probably would include modification of the lake's outlets, possibly including a selective withdrawal tower. A diversion of water from the upper Tualatin River into Henry Hagg Lake (a "Sain Creek tunnel") is also under consideration, as normal annual rainfall in the basin is not enough to fill the increased volume of an enlarged Henry Hagg Lake (Montgomery Watson Harza, 2004). The effects of these proposed structural changes on lake water quality, and the quality of water withdrawn and released from an enlarged lake are important, yet unknown.

Purpose and Scope

The purpose of this study was to develop a model of Henry Hagg Lake that can (1) simulate the circulation, temperature, and water quality in the lake, (2) aid in developing a more in-depth understanding of lake circulation and quality and the processes affecting them, and (3) predict the changes in circulation, temperature, and quality that might result from a suite of proposed dam modifications. This report addresses the first two goals.

The model was constructed to simulate conditions that occurred from 2000 through 2003. Model calibration focussed on the years 2000 and 2001; the calibrated model was tested with data from 2002 and 2003. Hydrologic conditions during this period were variable, from near-normal conditions in most years to extreme drought conditions in winter 2000–01, which caused the lake to only reach approximately 50% of storage capacity in 2001. A sensitivity analysis was conducted to better understand the model's response to some of its most important parameters or inputs.

This investigation resulted from a scientific and financial partnership between the U.S. Geological Survey (USGS) and CWS, one of a group of agencies investigating the various options for meeting future water-supply needs in the Tualatin River Basin.

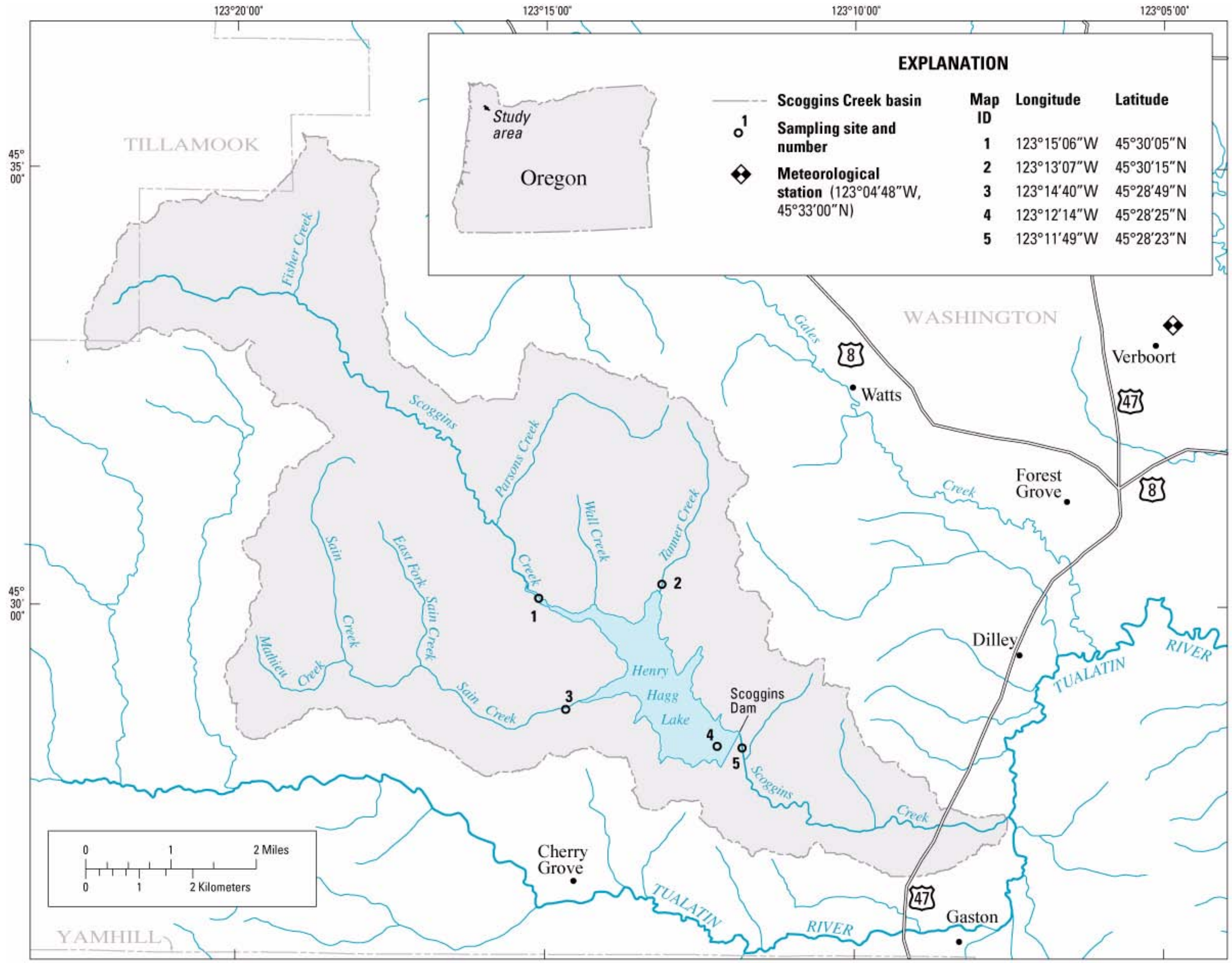

Figure 1. Henry Hagg Lake, Oregon, showing locations of data-collection sites.

Previous Work

Knutson (1993) constructed a model of Henry Hagg Lake for the summer of 1990 with an earlier version of CE-QUAL-W2. Streamflow data for inflows and outflows were available, but no temperature or water-quality data were available for the tributaries, and only limited data were available to characterize or calibrate water quality in the lake. Estrada (2000) studied algal communities and analyzed some water-quality constituents in the reservoir as part of a comparison of Henry Hagg Lake and Barney Reservoir, a man-made lake to the west of Henry Hagg Lake on the Trask River.

Methods

Model Description

The Henry Hagg Lake model was constructed using CE-QUAL-W2 version 3.12 (Cole and Wells, 2002), a two-dimensional hydrodynamic and water-quality model developed by the U.S. Army Corps of Engineers (USACE). This model is capable of simulating water levels, velocities, temperature, and water-quality constituents, including inorganic suspended solids, total dissolved solids, particulate and dissolved organic matter, pH, inorganic carbon, algae, silica, iron, dissolved oxygen, nitrogen, and phosphorus. Zooplankton dynamics were added to the CE-QUAL-W2 code used for the Henry Hagg Lake model based on modified zooplankton code from CE-QUAL-R1, the one-dimensional USACE lake water-quality model. These zooplankton algorithms may be included in a future version of CE-QUAL-W2. For the purposes of this report, they are documented in Appendix 1.

The model was developed in several steps. First, a model grid was constructed based on available lake bathymetry data. Input data were specified for an upstream boundary, for tributaries, distributed tributaries, withdrawals, and meteorological conditions. The model water budget was calibrated by comparing measured and predicted lake stage. Finally, the model was calibrated for temperature and water quality by comparing independently collected vertical profile data collected throughout each year to model output at the same date, time, and location.

The model was initially run and calibrated for January 1 to December 31, 2000, and for January 1 through December 31, 2001. After calibration was finalized, the model was tested (confirmed) for January 1 to December 31, 2002, and for January 1 to December 31, 2003. Further details on model development are discussed later in this report.

Bathymetry Data and the Model Grid

A CE-QUAL-W2 model grid is constructed from a series of model segments that are connected in the direction of flow. Each segment is divided into horizontal layers, and the widths of the layers are defined so that the cross section of a segment approximates a reservoir cross section. Segments are grouped together into one or more model branches to form the upstream to downstream backbone of the waterbody.

As a first step in developing the model grid, a Bureau of Reclamation digital elevation model (DEM) of Henry Hagg Lake's bathymetry below the full-pool water surface was combined with a DEM of the land above the current maximum water surface to produce a geographic information system (GIS) coverage with sufficient topographic data to examine the effects of raising the dam height by up to 12.2 m (40 ft). The Bureau of Reclamation DEM of the lake bathymetry was produced from a 2001 underwater survey using sonic depth recording equipment connected to a differential global positioning system (GPS) (Ferrari, 2001).

Using GIS, 45 cross-sections were extracted along lines drawn across the combined coverage perpendicular to the long axis of the reservoir at approximately 150 m intervals (fig. 2) to produce model segments. The bathymetry between those lines was determined by extracting eight intermediate cross sections. These cross sections were processed to provide averaged information for the model segments. Note that several of the cross-sectional lines shown in figure 2 were angled to better capture bathymetric information in two of the lake's arms. This slight misrepresentation of the lake's shape and orientation was used to capture all of the lake's volume without having to include additional branches in the model.

The final grid consisted of one model branch with inflows from Scoggins Creek and two other tributaries, Sain Creek and Tanner Creek. Without boundary segments and layers, the model grid consisted of 45 segments and 54 layers. Layer heights were 1 m each. The model grid was determined to accurately represent the reservoir bathymetry by comparing model volume-elevation and area-elevation curves to those determined from the survey (Bureau of Reclamation, 2001; Ferrari, 2001) (fig. 3). A two-branch model grid also was developed in which the Sain Creek arm of the lake was modeled with its own branch. Preliminary results from that model were not significantly different from the one-branch model, however, and further development of the two-branch model was discontinued due to run-time considerations when the Sain Creek branch became dry in late summer.

Other Model Data

Meteorological Data

Most of the meteorological data used in this study were obtained from the Bureau of Reclamation Agrimet station just north of Forest Grove (fig. 1). Global solar radiation was measured at this site with a pyranometer. Air temperature, rainfall, wind speed, wind direction, and relative humidity also were measured.

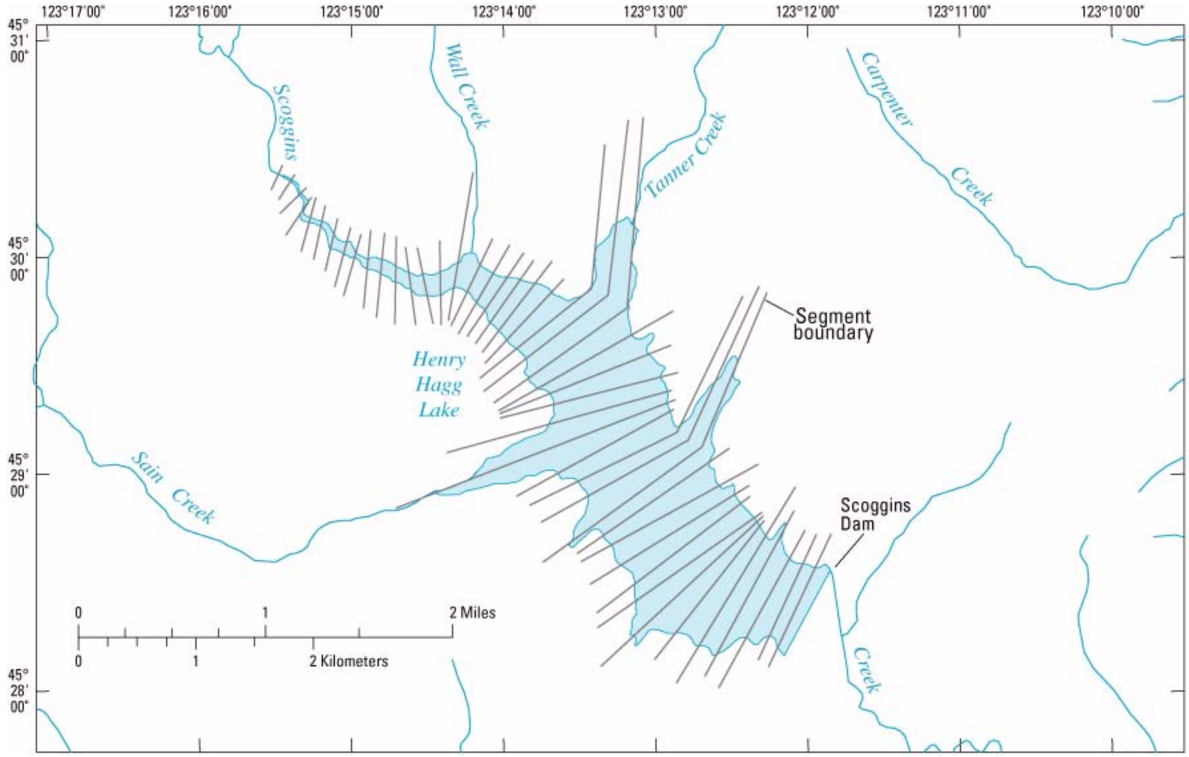

Figure 2. Location of segment boundaries for the model grid.

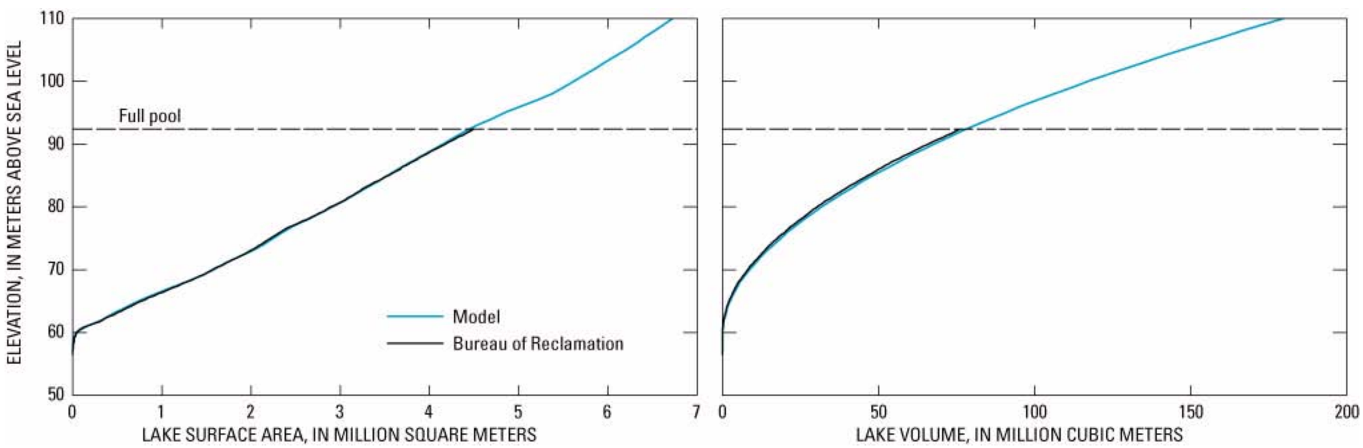

Figure 3. Volume-elevation and area-elevation curves for the model grid compared to results from the Bureau of Reclamation 2001 lake survey. The current full-pool elevation is noted (92.5 meters).

Dew point temperature was calculated from air temperature and relative humidity. Hourly data were used for model input.

In addition to precipitation measured at the Agrimet site, the Bureau of Reclamation measured daily precipitation at Scoggins Dam. Precipitation data were compared, and while minor differences were present, using one precipitation dataset over another did not appreciably change the water balance. The final model used the Scoggins Dam precipitation data. Air temperature was used as a surrogate for precipitation temperature.

Hydrological Data

The Oregon Water Resources Department (OWRD, District 18) monitored inflows to Henry Hagg Lake. Streamgages were located on the three largest tributary streams—Scoggins, Sain and Tanner Creeks (fig. 1). Figure 4 shows the inflows from these three tributaries for 2000 through 2003. Inflows at Scoggins and Sain Creeks were specified at 2-hour intervals; daily data were used for Tanner Creek. These flow data clearly illustrate the wet winters and dry summers that are characteristic of western Oregon. The below-normal rainfall and streamflow during the winter of 2000–01 also are noteworthy. The greatly reduced inflows to the lake during that period prevented the lake from filling prior to the summer of 2001.

The main outlet for Henry Hagg Lake draws water from a lake elevation of 69.8–72.5 m, approximately 14 m above the reservoir bottom. As part of flood control operations, water also can be released via the spillway, which has a crest elevation of 86.4 m. Radial gates control spillway releases and allow lake elevations as high as 93.2 m. Information on the elevation and dimensions of both of these withdrawal structures was included in the model. Total outflow data, combining the main outlet and spillway flows, were obtained from the USGS gage approximately 180 m downstream from Scoggins Dam (USGS station 14202980). Measured outflows from the reservoir for 2000–03 are shown in figure 4. Data provided by the dam operator were used to separate the total outflows into outlet and spillway flow for the model (Wally Otto, TVID, written comm., 2004).

The forebay water surface elevation of Henry Hagg Lake was continuously measured by the Bureau of Reclamation. This elevation was compared to the modeled lake forebay elevation and used to calibrate the water budget.

Water Temperature and Water-Quality Data

Tributary temperature and water-quality data were incorporated into the model. Temperature data were measured in Scoggins Creek above Henry Hagg Lake using continuous monitors for part of the period of interest. Water-quality samples were collected by personnel from the Joint Water Commission (JWC), who together with CWS started a 5-year water-quality monitoring program in Henry Hagg Lake in August of 1999. Samples were taken from the three main tributaries to the lake (Scoggins, Sain, and Tanner Creeks) approximately every month. Water temperature, pH, dissolved oxygen, specific conductance, and turbidity were measured in the field by JWC personnel. Samples for the analysis of total suspended solids, total phosphorus, orthophosphate, nitrate plus nitrite, total Kjeldahl nitrogen (TKN), and ammonia also were collected from the tributaries.

Water-quality samples were taken in Henry Hagg Lake at one location near the deepest part of the lake approximately monthly from November to April and twice a month from May to October. Vertical profiles of temperature, dissolved oxygen, pH, specific conductance, and turbidity were measured with a multiparameter probe (Hydrolab or YSI), and samples for nutrient analysis were obtained at specific depths in the lake with a Van Dorn sampler. Two nutrient samples were taken from each depth, and one was acidified with sulfuric acid. In addition, a chlorophyll *a* sample was taken from 1 m depth, and a sample for phytoplankton identification and enumeration was taken at the lake surface. Zooplankton samples were vertical integrations from 1 m off the bottom to the surface and were collected using a conical, 20-cm diameter plankton net.

The probe used to measure dissolved oxygen in Henry Hagg Lake and its tributaries malfunctioned during portions of 2002 and 2003. Plots of tributary temperature versus tributary dissolved oxygen showed that dissolved oxygen concentrations in previous years were consistently at or slightly below saturation. However, in parts of 2002 and most of 2003, the data plotted erratically well above or below the saturation line and trend of previous years. On the dates with erratic dissolved oxygen data, the measured data were discarded and tributary dissolved oxygen concentrations were estimated using the measured temperature and the dissolved oxygen-temperature relation from previous years. Most of the 2002 dissolved oxygen data appeared reasonable, so goodness-of-fit statistics for the modeled dissolved oxygen concentrations in the lake were calculated, but the possibility of erroneous dissolved oxygen measurements in the lake must be considered when examining those 2002 statistics. Measured lake profiles of dissolved oxygen were not compared to model output for 2003, due to the large number of erratic measurements.

Nutrient and chlorophyll samples were shipped to the Bureau of Reclamation laboratory in Boise, Idaho. That laboratory participates in the Standard Reference Sample quality assurance program administered by the USGS Branch of Quality Systems. Laboratory performance for these parameters has been excellent (see http://bqs.usgs.gov/srs/, lab #10); the chemical data should be sufficiently accurate for the purposes of this study. Unacidified samples were filtered in the laboratory with a 0.45 µm (micrometer) filter. Total phosphorus and orthophosphate were analyzed by U.S. Environmental Protection Agency (USEPA) method 365.1 (USEPA, 1993). Ammonia was analyzed by USEPA method 350.3 (USEPA, 1983). TKN was analyzed by USEPA method 351.2 (USEPA, 1983). Chlorophyll *a* was analyzed by Standard Methods 10200H (American Public Health Association, 1998).

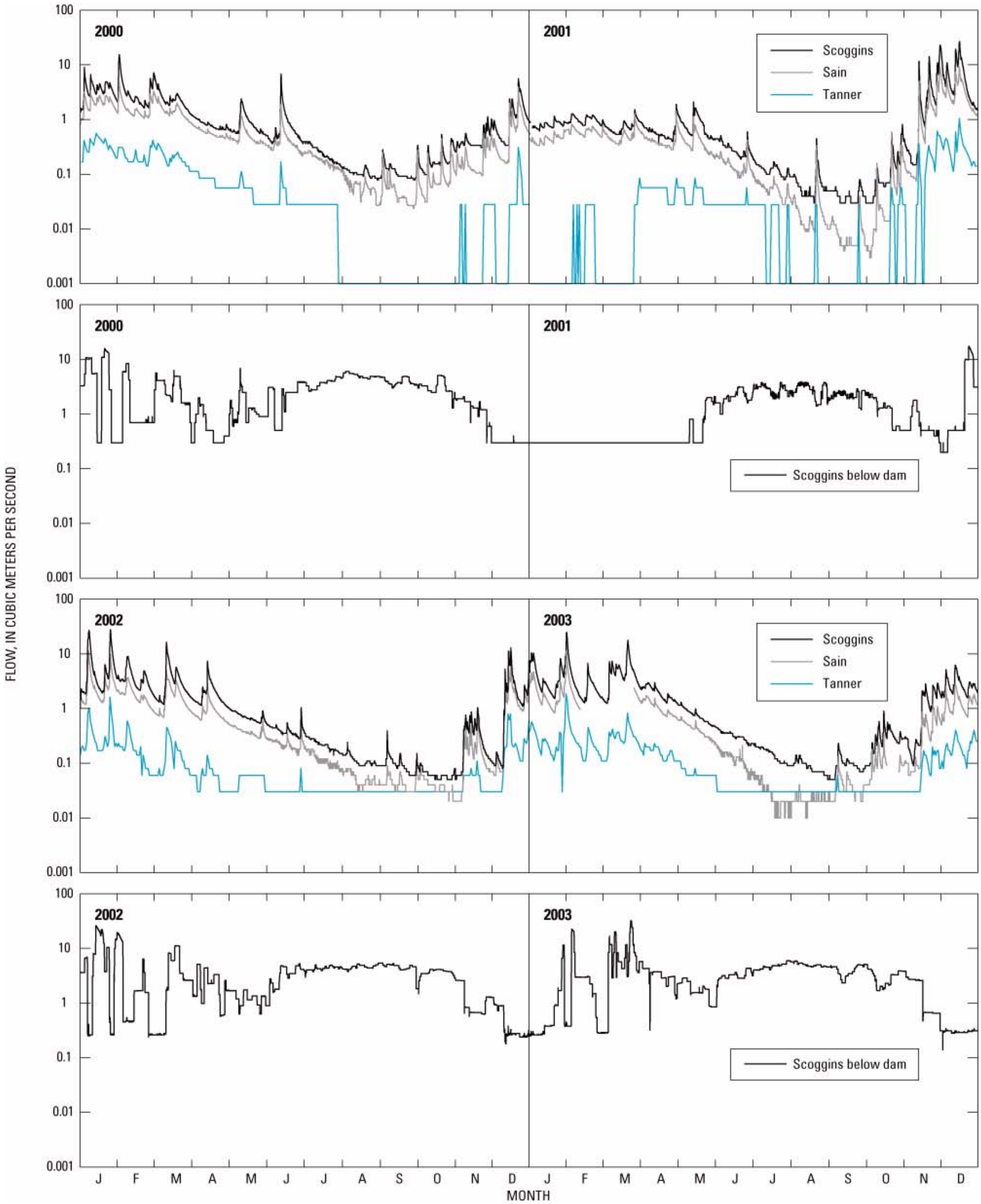

Figure 4. Measured tributary inflows to Henry Hagg Lake from Scoggins, Sain, and Tanner Creeks and flows in Scoggins Creek just downstream of the dam for 2000–03.

Phytoplankton species were identified and enumerated in each sample, and biovolumes and densities were computed. Likewise, for zooplankton samples, species were identified, and species density and biovolumes were calculated. The distribution of zooplankton lengths also was determined. Most of these data are available online in the annual reports of the Tualatin River flow management technical committee (Tualatin River Flow Management Technical Committee, 2000 to 2003).

In addition to the sampling program carried out by the JWC, the USGS also collected data from Henry Hagg Lake in August and September 2003, and September 2004. Profiles of temperature, dissolved oxygen, specific conductance, pH, turbidity, and light were collected near the dam and also at additional locations in the reservoir, including the Sain Creek arm. Nutrient samples also were collected by USGS and analyzed by CWS (http://bqs.usgs.gov/srs/, lab #180). This sampling was completed to confirm that lateral differences in water quality were minor, to measure light extinction coefficients, and to obtain in-lake nitrate data, which were not included in the JWC monitoring program.

Model Calibration

Water Balance

Initial model runs using only the three gaged tributaries did not have enough inflow to complete the water balance, thus revealing the presence of one or more ungaged inflows to the lake, such as ground-water discharge and flows from small tributaries. The model allows for input of a distributed tributary that accounts for these ungaged flows. The model does not treat them as point-source inflows; instead they are “distributed” along an entire model branch. The distributed tributary inflow varied significantly seasonally. For instance in 2000, the beginning of the drought, 100% of the distributed tributary inflow occurred from January through April and November to December. During summer, no distributed tributary inflow occurred; instead, a loss of water was discovered—that is, lake water was lost to the sediments. A similar situation occurred in 2001, though the summer loss was smaller. In both 2002 and 2003, 88% of the distributed tributary inflows occurred during the rainy periods from January through April and November through December, and no significant summertime loss of water was detected. Considering both distributed tributary inflows and losses, the annual proportion of the distributed tributary input was 6% of the total annual inflows in 2000, 16% in 2001, 19% in 2002, and 30% in 2003. It is not known with certainty why the distributed tributary input was relatively large in 2003, as annual inflows were similar in both 2002 and 2003. It is possible that physical changes to the streambed at gage stations (from storm events, for example) affected the relation between stage and flow on tributaries between years, thus increasing the measurement error. Results of the final water calibration for 2000 through 2003 are shown in figure 5.

Henry Hagg Lake water surface elevations are typically managed according to a fill curve (fig. 5). The lake is drawn down in early winter to provide for flood control. The fill curve allows the lake to capture approximately 20,600 acre-feet of flood water from the upper Scoggins Creek drainage. The lake typically is filled by May to maximize storage of water for summertime use by agricultural, municipal, and other water-right holders. Releases of water for downstream uses causes the water surface elevation to decrease through the summer; the lowest water surface elevation typically occurred in November during this study. In December, the reservoir begins to fill again as withdrawals decrease and winter storm flows are captured. Precipitation and runoff in winter 2000 to spring 2001 was abnormally low, and the reservoir did not fill. The highest lake level in 2001 was approximately 7.5 m lower than the highest lake level in 2000. At its lowest point in 2001, the lake elevation was only 2.4 m above the main outlet structure—the lowest stage recorded since construction of Scoggins Dam.

Water Temperature

Water temperature in reservoirs is affected by inflows and outflows, exchange of heat at the air-water interface (short- and long-wavelength radiative inputs, long-wavelength radiative emissions, evaporation, conduction, and convection), depth penetration by solar radiation, and mixing by wind. In the model, water temperature was initialized with temperature measured near January 1, when the lake was isothermal and well-mixed. Modeled water temperature was affected by the lake’s energy balance and circulation, as well as parameters such as the light extinction coefficient. Water temperature calibration was completed by adjusting model parameters to achieve reasonable agreement between measured and modeled water temperature at the depth-profile sampling location near the deepest part of Henry Hagg Lake (fig. 1). Some of the final calibrated model parameters relevant to the simulation of water temperature are listed in table 1.

The overall temperature cycle in Henry Hagg Lake was consistent in the 4 years simulated in this study, including 2001, the year in which the reservoir did not fill. Comparison of measured and modeled temperature profiles at the same location, date, and time for 2000 through 2003 are shown in figures 6–9. Modeled temperature near the dam is also shown for an entire year (2002) in figure 10. From December through February, Henry Hagg Lake typically was isothermal and cold. Surface temperatures began to warm in March due to increased solar radiation, and by mid-May to June a thermocline developed at depths between 5 and 15 m, and persisted until October-November. This distinct vertical temperature gradient develops in the summer due to the absorption of solar and atmospheric radiation in the upper part of the lake’s water column. Warmer water is less dense than the cooler water below it, which tends to deter vertical mixing processes and strengthen the temperature gradient.

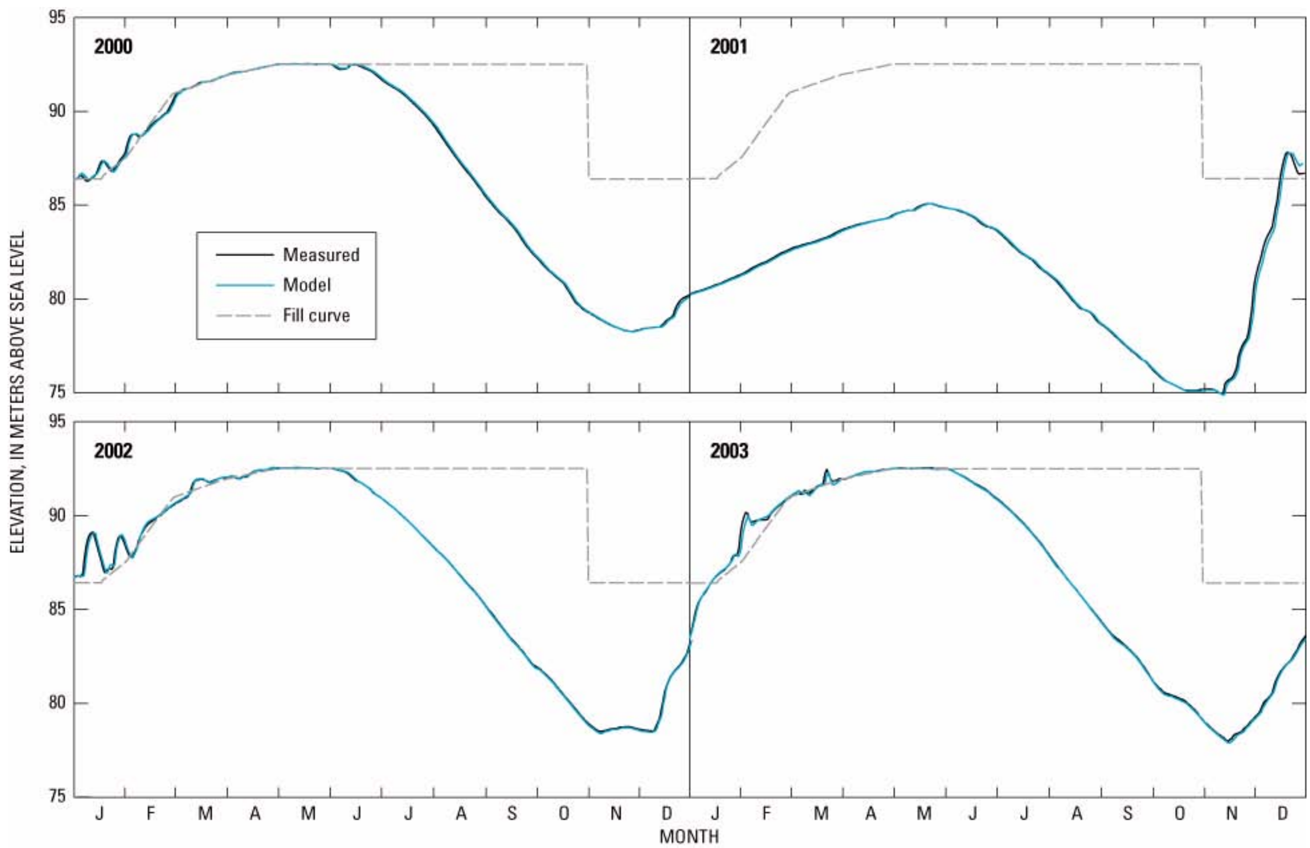

Figure 5. Henry Hagg Lake forebay elevation measured by the Bureau of Reclamation and the calibrated Henry Hagg Lake water surface elevation for the model for 2000 through 2003. The fill curve is shown for comparison.

In Henry Hagg Lake, temperature decreased as much as 12ºC over 5 m (18ºC over 10 m) depth through the thermocline. As withdrawals increased in summer, the lake stage decreased, causing the thermocline to move downward towards the withdrawal outlet elevation. The density difference between the warmer surface water in the epilimnion and the denser colder water in the hypolimnion isolated the water below the reservoir outlet in summer. Later in the year, as solar radiation and air temperature decreased, the temperature of the lake surface cooled, and eventually the density of the surface and deep waters were similar enough to allow the lake to "turn over" and mix, becoming isothermal again. This classic limnological cycle occurred in all years simulated in this study.

The model also can simulate the temperature of water discharged from the reservoir. This model-predicted outflow temperature is compared to available water temperature data from Scoggins Creek approximately 180 m downstream of the dam in figure 11. The modeled and measured results matched well; the small differences were likely due to air-water heat exchange processes occurring between the reservoir outlet and the downstream measuring location on Scoggins Creek, as the water is energetically and efficiently aerated upon release from the dam.

Calculation of goodness-of-fit statistics for the comparison of modeled and measured temperature profiles produced annual mean errors (ME) between -0.22 and +0.05ºC, mean absolute errors (MAE) between 0.62 and 0.68ºC, and root mean square errors (RMSE) between 0.86 and 0.94ºC for 2000 through 2003 (table 2). The range of these goodness-of-fit statistics was similar for the calibration period (2000–01) and for the confirmation period (2002–03), demonstrating that the temperature calibration was relatively robust. The fact that the ME is near zero and the MAE and RMSE show errors of less than 1ºC indicates that the model accurately captured the energy budget and thermal characteristics of Henry Hagg Lake.

Water Quality

The model was calibrated for orthophosphate, total phosphorus, ammonia, chlorophyll *a*, algal biovolume, zooplankton biovolume, and dissolved oxygen with available measured data. Some constituents, organic carbon and nitrate for example, were included in the model with little measured data for calibration, because they were important in the cycles of other constituents. pH was not simulated due to a lack of alkalinity data; simulating pH could be a future modeling task. Calibration consisted of setting model parameters to literature values or to values used by other models (e.g., Cole and Wells, 2002; Bowie et al., 1985; Rounds et al., 1999) and refining them in a logical and organized fashion until modeled and measured concentrations matched reasonably well.

Table 1. Model parameters and values used in the Henry Hagg Lake model.

[m, meter; g, gram; ºC, degrees Celsius; W, Watts; sec, second]

Parameter	Value	Description
WSC	1.0	Wind sheltering coefficient, dimensionless
EXH2O	0.25	Light extinction coefficient for pure water, 1/m
EXSS	0.01	Light extinction due to inorganic suspended solids, m^2/g
EXOM	0.08	Light extinction due to organic suspended solids, m^2/g
EXA	0.20	Light extinction due to algae, m^2/g
BETA	0.53	Fraction of solar radiation absorbed at water surface, dimensionless
TSED	11.2	Sediment temperature, ºC
CBHE	0.879	Coefficient of bottom heat exchange, $W/m^2/sec$
LDOMDK	0.03	Labile dissolved organic matter decay rate, 1/day
RDOMDK	0.005	Refractory dissolved organic matter decay rate, 1/day
LRDDK	0.001	Labile to refractory dissolved organic matter conversion rate, 1/day
LPOMDK	0.01	Labile particulate organic matter decay rate, 1/day
RPOMDK	0.002	Refractory particulate organic matter decay rate, 1/day
LRPDK	0.001	Labile to refractory particulate organic matter conversion rate, 1/day
POMS	0.08	Particulate organic matter settling rate, m/day
OMT1	4.0	Lower temperature parameter for organic matter decay, ºC
OMT2	30.0	Upper temperature parameter for organic matter decay, ºC
OMK1	0.1	Fraction of organic matter decay rate at OMT1
OMK2	0.99	Fraction of organic matter decay rate at OMT2
ORGP	0.004	Stoichiometric equivalent between organic matter and phosphorus, g P/g OM
ORGN	0.08	Stoichiometric equivalent between organic matter and nitrogen, g N/g OM
ORGC	0.45	Stoichiometric equivalent between organic matter and carbon, g C/g OM
PARTP	0.0	Phosphorus partitioning coefficient for suspended solids, dimensionless
PO4R	0.004	Release rate of phosphorus from sediment, as a fraction of SOD
NH4R	0.037	Release rate of ammonium, as a fraction of SOD
NH4DK	0.12	Ammonia nitrification rate, 1/day
NH4T1	4.0	Lower temperature parameter for ammonia nitrification, ºC
NH4T2	25.0	Upper temperature parameter for ammonia nitrification, ºC
NH4K1	0.10	Fraction of nitrification rate at NH4T1
NH4K2	0.99	Fraction of nitrification rate at NH4T2
NO3DK	0.10	Denitrification rate, 1/day
NO3S	0.2	Denitrification rate, loss to sediments, m/day
NO3T1	5.0	Lower temperature parameter for nitrate denitrification, ºC
NO3T2	25.0	Upper temperature parameter for nitrate denitrification, ºC
NO3K1	0.01	Fraction of denitrification rate at NO3T1
NO3K2	0.99	Fraction of denitrification rate at NO3T2
O2NH4	4.33	Oxygen stoichiometry for nitrification, g O_2/g N
O2OM	1.40	Oxygen stoichiometry for organic matter decay, g O_2/g OM
O2AR	1.10	Oxygen stoichiometry for algal respiration, g O_2/g algae
O2AG	1.40	Oxygen stoichiometry for algal primary production, g O_2/g algae
O2LIM	0.01	Dissolved oxygen concentration at which anaerobic processes begin, g/m^3
O2ZR	1.1	Stoichiometric coefficient for the production of oxygen from zooplankton respiration, g O_2/g zooplankton
SEDCI	0.0	Initial sediment concentration, g/m^2
SDK	0.02	Sediment decay rate, 1/day
SODT1	4.0	Lower temperature parameter for zero-order SOD or first-order sediment decay, ºC
SODT2	30.0	Upper temperature parameter for zero-order SOD or first-order sediment decay, ºC
SODK1	0.14	Fraction of SOD or sediment decay rate at SODT1
SODK2	0.88	Fraction of SOD or sediment decay rate at SODT2
SOD	2.0	Zero-order sediment oxygen demand (SOD) for each segment, g O_2/m^2/day
SSS	0.5	Suspended solids settling rate, m/day

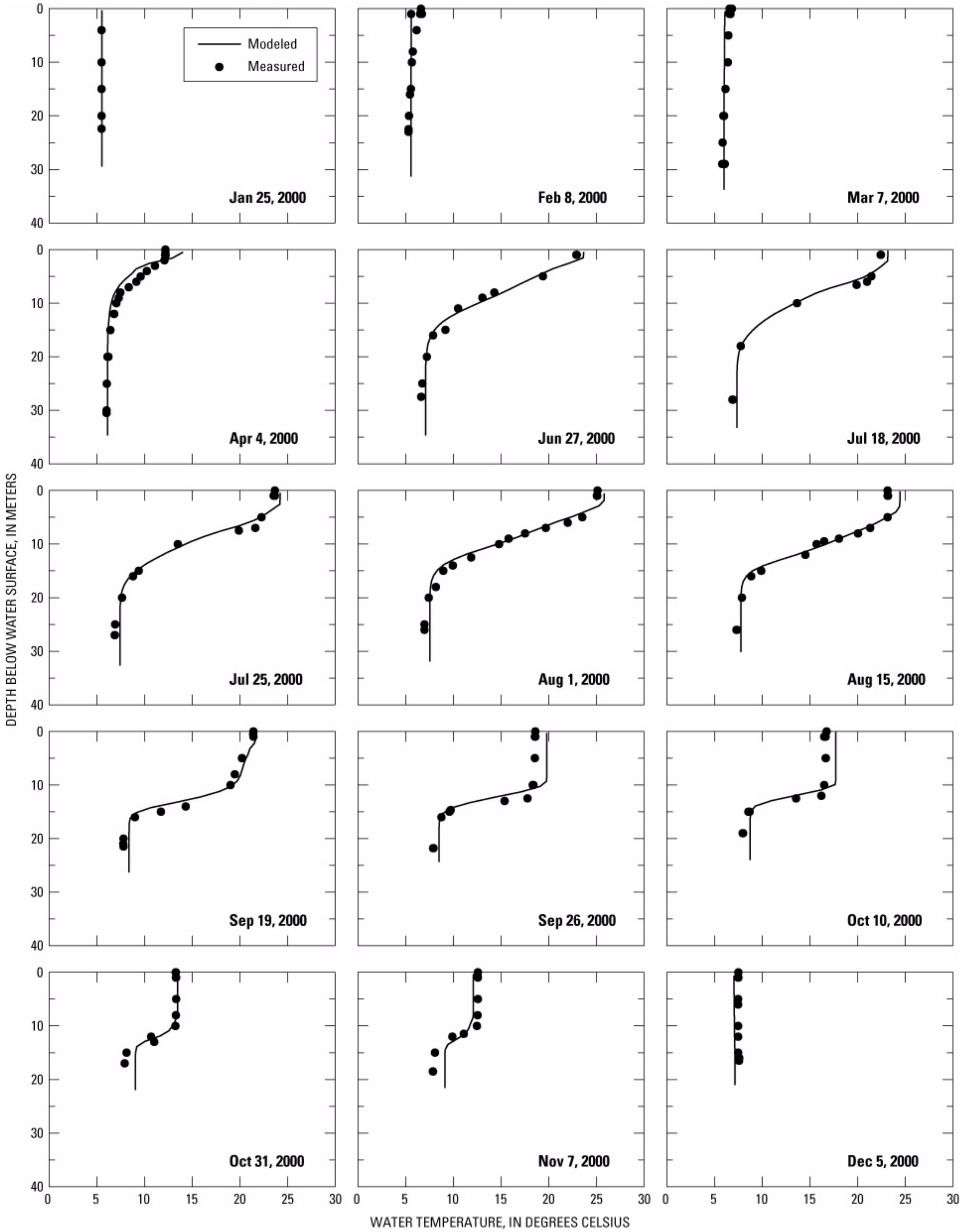

Figure 6. Measured water temperature profiles in the deepest part of the lake near the dam compared to modeled values from the same location and the same time in 2000.

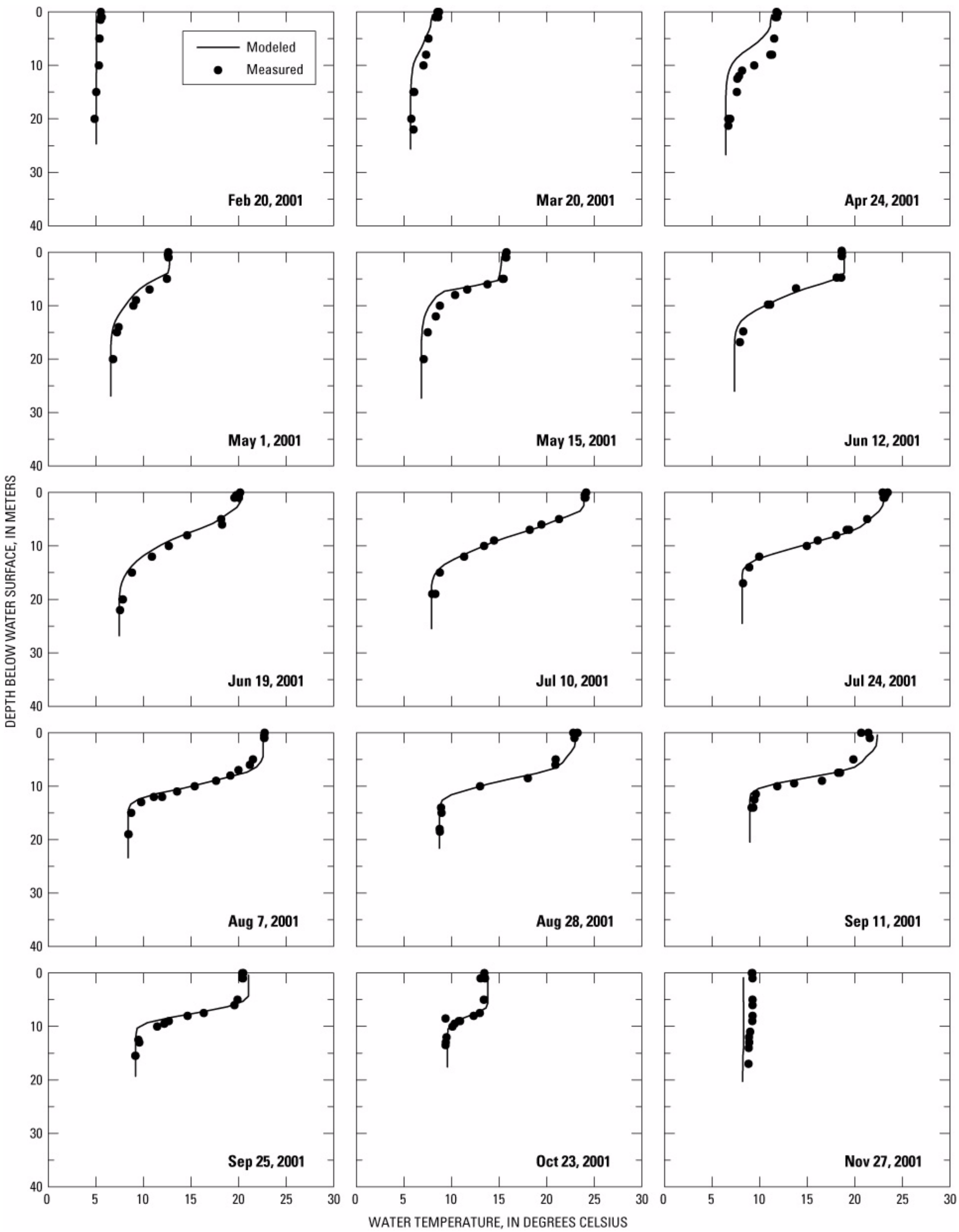

Figure 7. Measured water temperature profiles in the deepest part of the lake near the dam compared to modeled values from the same location and the same time in 2001.

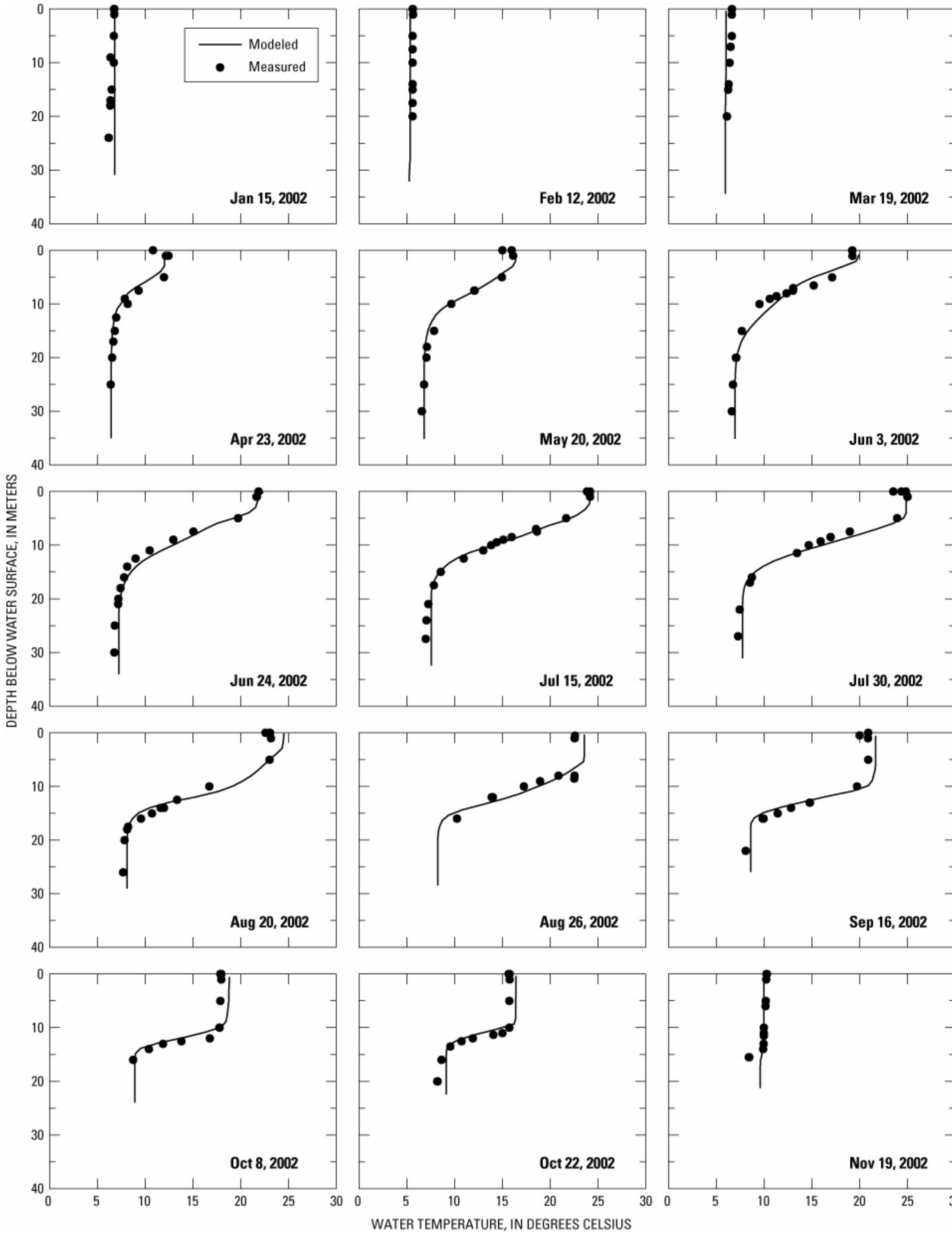

Figure 8. Measured water temperature profiles in the deepest part of the lake near the dam compared to modeled values from the same location and the same time in 2002.

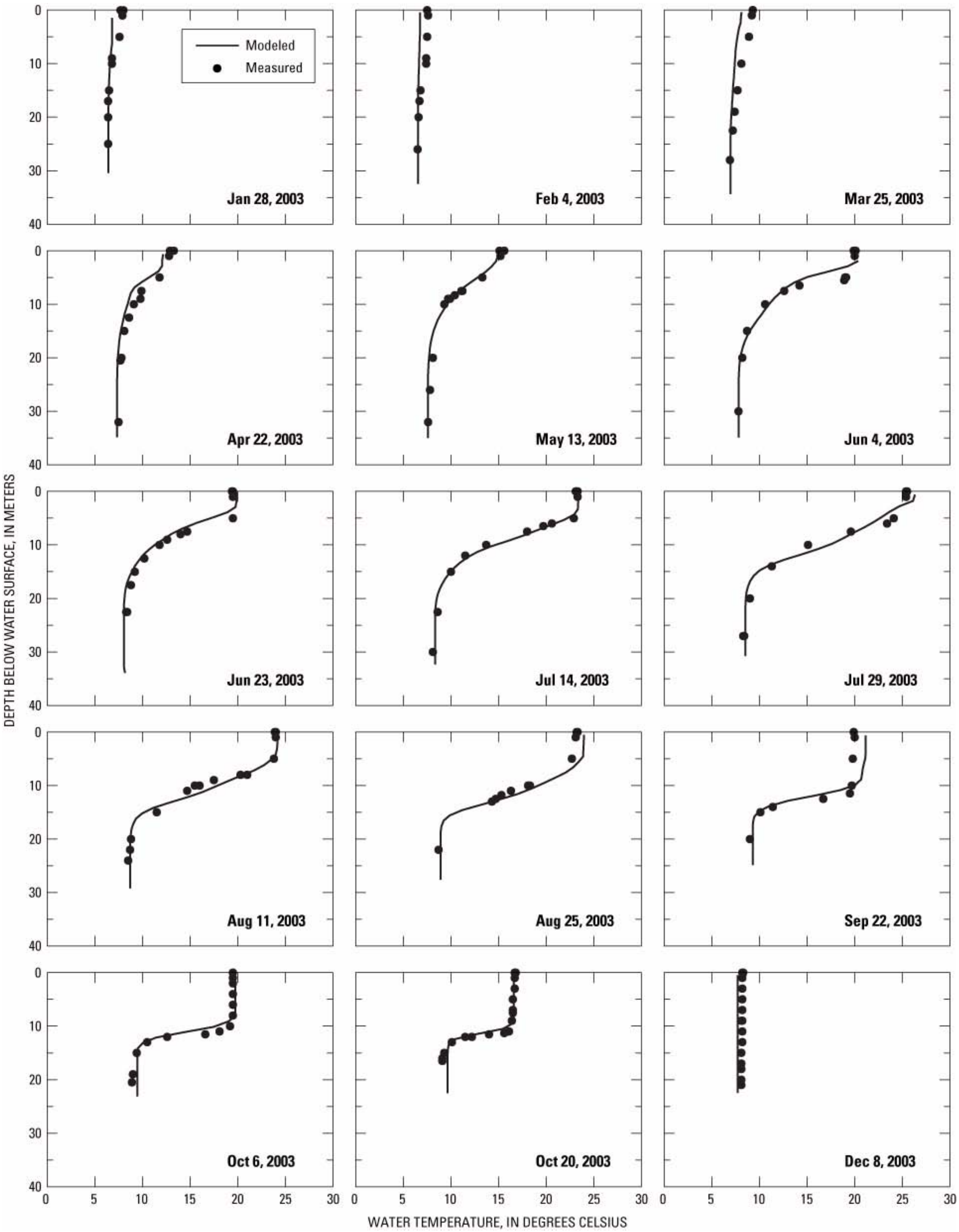

Figure 9. Measured water temperature profiles in the deepest part of the lake near the dam compared to modeled values from the same location and the same time in 2003.

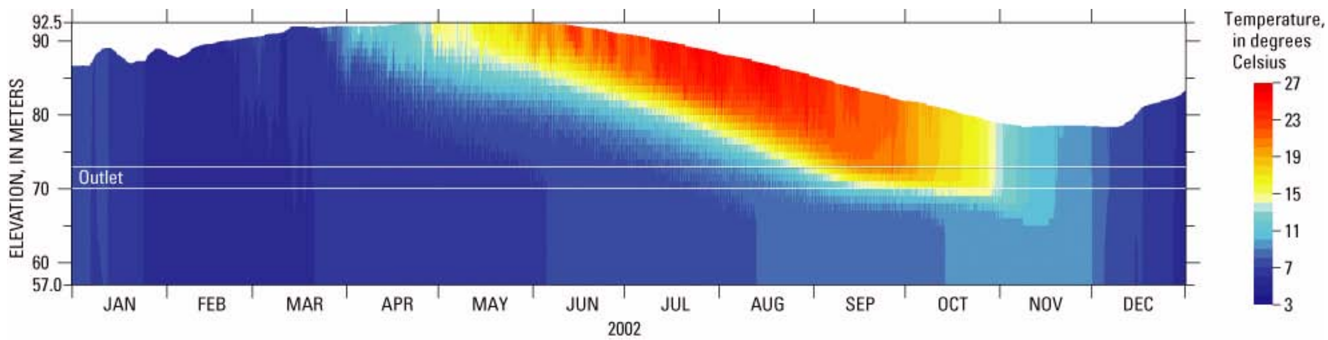

Figure 10. Modeled water temperature in the deepest part of the lake near the dam in 2002. The elevation range of the lake outlet is noted by the two horizontal lines at elevations of 69.8 and 72.5 meters.

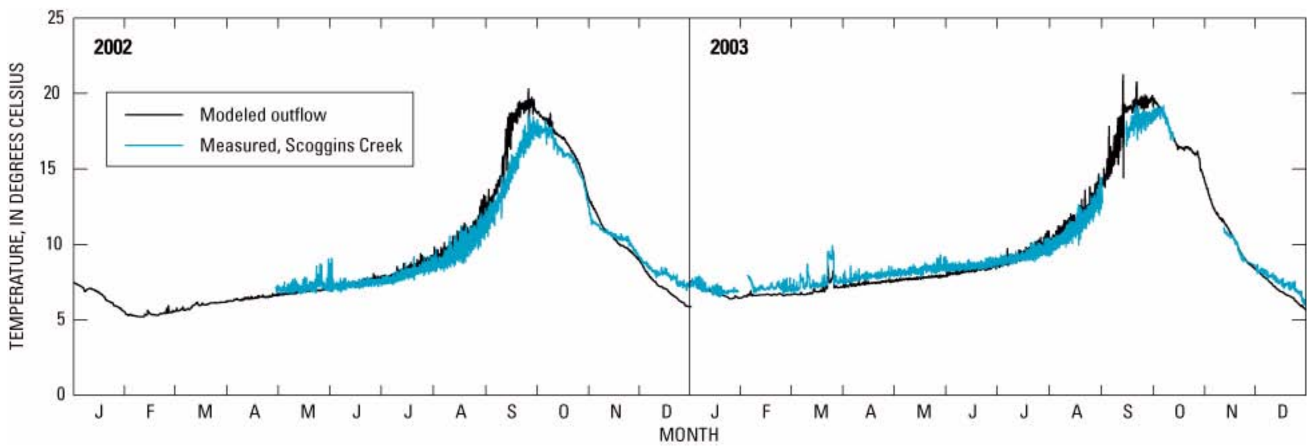

Figure 11. Comparison of modeled water temperature of the reservoir outflow to measured water temperature in Scoggins Creek 180 meters downstream of the dam at USGS station 14202980.

The water-quality constituents in this type of model are highly interconnected, and small changes to one can have a large effect on others. Because most of the simulated water-quality processes are necessarily simplified representations of complex chemical and biological reactions, the overall goal of model calibration was to capture the essence of the most important processes at their relevant spatial and temporal scales. Acceptance of some amount of error is inevitable; the iterative process of model parameter adjustment aimed to minimize the errors while preserving the model's descriptive and predictive abilities.

As with temperature, the model was only run for 1 year at a time, and the water-quality constituents in the model were initialized each year with measured values taken on or about January 1. For most of the modeled constituents (e.g., temperature, dissolved oxygen, ammonia), the modeled concentration from the end of the previous year was not particularly different from the measured concentration used to initiate the next year's model run; therefore, this practice did not mask any carryover of error from year to year. For a few constituents (e.g., zooplankton), the agreement was less favorable, but still acceptable. Because it was more important to examine processes, trends, seasonal variations, and other dynamics of water quality on time scales of less than a year (rather than to create a decade-scale predictive tool), the decision to initialize the model each year with measured values was the best option.

Orthophosphate and Total Phosphorus

Phosphorus is an essential nutrient in a lake's ecological web. Orthophosphate (PO_4^{3-}) can be rapidly utilized by actively growing phytoplankton in the lake's epilimnion and can increase particulate phosphorus concentrations as the algal biomass grows. Later, bacterial decomposition of dead cells, and other processes, including zooplankton excretions, can release soluble and particulate forms of phosphorus to the water column, some of which are biologically available. In the Henry Hagg Lake model, sources of orthophosphate included inputs from the tributaries; algal and zooplankton respiration; decay of dissolved, suspended, and sedimentary organic matter; and anaerobic release from the lake sediments. Sinks included algal uptake and settling of particles containing or adsorbing phosphorus.

Table 2. Henry Hagg Lake model goodness-of-fit statistics for 2000–03. In this analysis, measured values below the detection limit were assumed to be half of the detection limit.

[°C, degrees Celsius; mg/L, milligrams per liter; µg/L, micrograms per liter]

	Calibration		Confirmation	
	2000	**2001**	**2002**	**2003**
Mean Error				
Temperature (°C)	-0.04	-0.22	0.05	-0.14
Ortho-P (mg/L as P)	0.002	0.001	0.003	0.004
Total P (mg/L as P)	-0.007	-0.001	-0.004	0.003
Ammonia (mg/L as N)	0.00	0.00	0.00	0.01
Chlorophyll *a* (µg/L)	-0.3	-2.3	-2.0	-1.2
Dissolved Oxygen (mg/L)	0.18	0.09	-0.28	-
Mean Absolute Error				
Temperature (°C)	0.68	0.63	0.67	0.62
Ortho-P (mg/L as P)	0.004	0.002	0.004	0.004
Total P (mg/L as P)	0.012	0.006	0.008	0.009
Ammonia (mg/L as N)	0.02	0.02	0.01	0.02
Chlorophyll *a* (µg/L)	1.9	2.3	2.4	2.1
Dissolved Oxygen (mg/L)	0.73	0.43	0.92	-
Root Mean Square Error				
Temperature (°C)	0.90	0.86	0.89	0.94
Ortho-P (mg/L as P)	0.007	0.003	0.005	0.007
Total P (mg/L as P)	0.019	0.010	0.010	0.011
Ammonia (mg/L as N)	0.05	0.03	0.04	0.03
Chlorophyll *a* (µg/L)	2.3	2.9	3.2	2.6
Dissolved Oxygen (mg/L)	0.91	0.60	1.24	-

Interaction of phosphorus with solid surfaces such as iron oxides can be important in removing dissolved phosphorus from the water column in lakes. While the anaerobic release of phosphorus from sediments can simulate dissolution and desorption of phosphorus from bed sediment solids, interactions of phosphorus with suspended particles or other solids were not included in the model. Some model parameters related to phosphorus and their values used in the calibrated model are listed in tables 1 and 3.

Modeled and measured orthophosphate and total phosphorus profiles at the same location, date, and time for a representative year (2002) are shown in figure 12. Modeled orthophosphate concentrations near the dam throughout 2002 are shown in figure 13. Phosphorus levels in the lake were low overall (total phosphorus typically <0.03 mg/L, orthophosphate typically <0.01 mg/L as P) relative to streams in the valley of the Tualatin Basin. The greatest deviation between modeled and measured phosphorus concentrations in Henry Hagg Lake typically occurred in the fall, when the model predicted higher orthophosphate and total phosphorus in the hypolimnion than was measured. This may have been due to a sampling artifact, involving precipitation of iron-phosphorus solids prior to filtration and analysis, that caused measured dissolved phosphorus concentrations to be artificially low. Water samples for phosphorus analysis taken from the anoxic hypolimnion in late September and October were brought to the surface, where upon exposure to oxygen (from the transfer of water from the Van Dorn to the sample bottles or due to the permeation of atmospheric oxygen through the plastic sample bottles), dissolved iron could have precipitated as solids and adsorbed some of the sample's phosphorus, leading to lower measured values than were actually present in the anoxic lake hypolimnion. During a USGS sampling in September 2004, precipitation of rust colored material (probably iron oxyhydroxide solids) was observed in a water sample from the lake hypolimnion within several hours after collection.

The temporal and vertical patterns in figures 12 and 13 illustrate several important processes affecting phosphorus concentrations in Henry Hagg Lake. First, the overall phosphorus concentrations were fairly low and typical of an oligotrophic system; the low phosphorus concentrations could be limiting algal growth and primary productivity. Second, when algal blooms occurred (late spring through summer), orthophosphate concentrations (the bioavailable phosphorus) decreased to levels below detection near the surface of the lake where the algae were growing.

Table 3. Algae and zooplankton parameters and values used in the Henry Hagg Lake model.

[m, meter; g, gram; W, Watts; °C, degrees Celsius]

Parameter	General algae	Blue-green algae	Zooplankton	Description
AG, ZG	2.7	9.0	0.40	Maximum algal growth or zooplankton grazing rate, 1/day
AR, ZR	0.03	0.01	0.01	Maximum respiration rate, 1/day
AE	0.03	0.01	-	Maximum algal excretion rate, 1/day
AM, ZM	0.0	0.0	0.001	Maximum nonpredatory algal mortality and maximum zooplankton mortality rates, 1/day
AS, ZS	0.10	-0.10	-0.02	Settling rate, m/day
AHSP	0.004	0.002	-	Algal half-saturation for phosphorus limited growth, g/m^3
AHSN	0.014	0.0	-	Algal half-saturation for nitrogen limited growth, g/m^3
ZHSF	-	-	0.15	Zooplankton half-saturation constant for food, g/m^3
ASAT	20	25	-	Light saturation intensity at maximum photosynthetic rate, W/m^2
AT1, ZT1	5	24	5	Lower temperature parameter for rising rate function, ºC
AT2, ZT2	10	24.5	18	Upper temperature parameter for rising rate function, ºC
AT3, ZT3	18	26.5	24	Lower temperature parameter for falling rate function, ºC
AT4, ZT4	24	29	30	Upper temperature parameter for falling rate function, ºC
AK1, ZK1	0.04	0.10	0.03	Fraction of rate at T1
AK2, ZK2	0.99	0.99	0.95	Fraction of rate at T2
AK3, ZK3	0.99	0.99	0.95	Fraction of rate at T3
AK4, ZK4	0.10	0.10	0.10	Fraction of rate at T4
AP, ZP	0.004	0.004	0.003	Stoichiometric equivalent between biomass and phosphorus, g P/g OM
AN, ZN	0.08	0.08	0.08	Stoichiometric equivalent between biomass and nitrogen, g N/g OM
AC, ZC	0.45	0.45	0.45	Stoichiometric equivalent between biomass and carbon, g C/g OM
ACHLA	90	220	-	Ratio between algal biomass and chlorophyll *a*
APOM	0.8	0.8	-	Fraction of algal biomass converted to particulate organic matter when algae die
ANPR	0.02	0.02	-	Algal half-saturation preference constant for ammonium
ZGEFF	-	-	0.85	Zooplankton grazing efficiency
ZPFA	0.55	0.03	-	Zooplankton preference factor for algae as food
ZPFPOM	-	-	0.55	Zooplankton preference factor for particulate organic matter as food
ZFMIN	-	-	0.02	Zooplankton feeding minimum threshold concentration, g/m^3
ZOOMIN	-	-	0.001	Zooplankton minimum population concentration, g/m^3

Lastly, when the lake's hypolimnion was anoxic from late August or September through mid-November, phosphorus concentrations increased near the lake bottom—a typical result of the dissolution of iron oxides in the lake sediments. This last trend is not always apparent in the measured data due to the possible artifact mentioned previously. Ammonia should also be released from the sediments under anoxic conditions, and this was in fact observed in the ammonia data each year.

Calculating goodness-of-fit statistics between measured and modeled orthophosphate produced annual MEs between 0.001 and 0.004 mg/L, MAEs between 0.002 to 0.004 mg/L, and RMSEs between 0.003 and 0.007 mg/L for 2000 through 2003 (table 2). For total phosphorus, annual MEs ranged from -0.007 to 0.003 mg/L, MAEs ranged between 0.006 and 0.012 mg/L, and RMSEs were between 0.010 and 0.019 mg/L. These statistics were small in part because the concentrations in the lake were low. The analytical accuracy of phosphorus measurements from a good laboratory typically are in the range of ±10% for orthophosphate and ±20% for total phosphorus, perhaps greater when concentrations are near the detection limit. Accounting for this level of analytical uncertainty, the comparison of measured and modeled phosphorus concentrations in figure 12 and table 2 is reasonable. The model kept track of the phosphorus relatively well, and with sufficient accuracy to meet the needs of this investigation.

Ammonia and Nitrate

Like phosphorus, nitrogen also is essential to a lake's biological productivity. While nitrogen gas (N_2) is the most common form of nitrogen in aquatic systems (Horne and Goldman, 1994), it is only usable by select bacteria, including some blue-green algae (cyanobacteria) capable of nitrogen fixation.

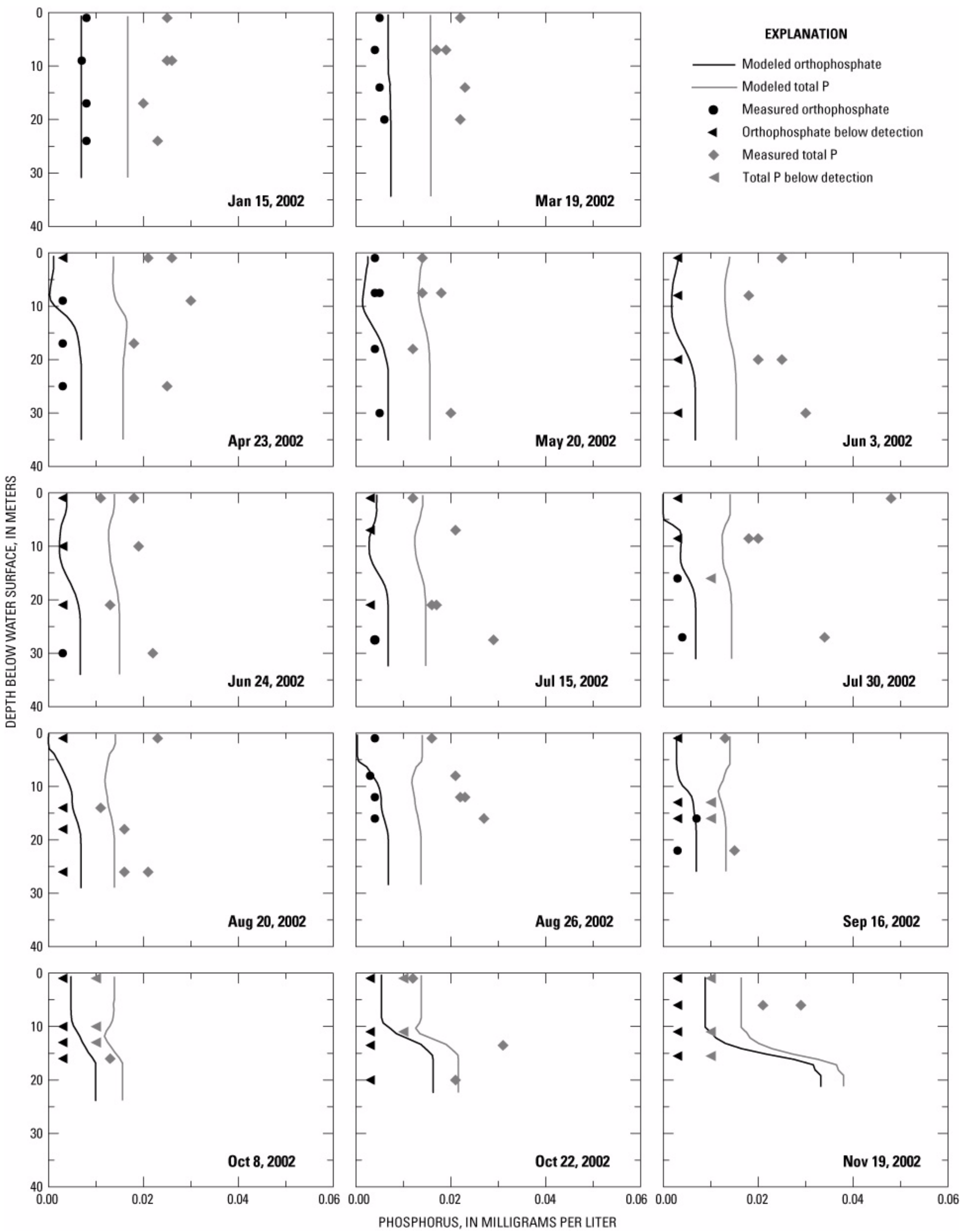

Figure 12. Measured orthophosphate and total phosphorus profiles in the deepest part of the lake near the dam compared to modeled values from the same location and the same time in 2002. The detection limit was 0.003 milligrams per liter as P for orthophosphate and 0.01 milligrams per liter for total phosphorus.

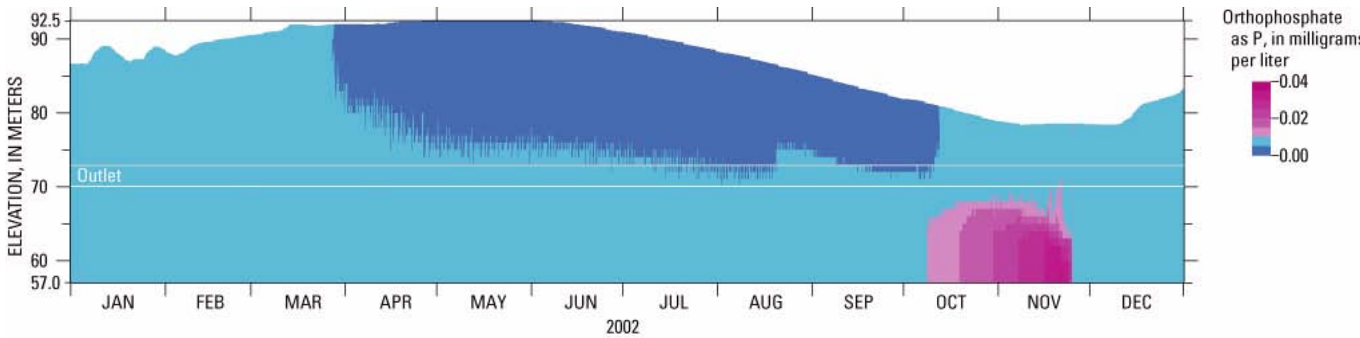

Figure 13. Modeled orthophosphate concentrations in the deepest part of the lake near the dam in 2002. The elevation range of the lake outlet is noted by the two horizontal lines at elevations of 69.8 and 72.5 meters.

Nitrate (NO_3^-) and ammonia (NH_3) are the more commonly utilized and measured aqueous nitrogen species. In this report, "ammonia" is used to refer to both NH_4^+ (ammonium) and NH_3. Uptake of these soluble forms of nitrogen can greatly lower their concentrations in the photic zone of lakes during the spring and summer. In the fall and winter, tributary inflows, ground-water discharges, and reactions in lake sediments tend to increase nitrate and ammonia concentrations in lakes.

In the Henry Hagg Lake model, sources of ammonia included anaerobic sediment release, respiration of algae and zooplankton, decay of organic matter, and tributary inputs. Sinks of ammonia included algal growth and conversion to nitrate via nitrification. Sources of nitrate included nitrification of ammonia, while sinks included denitrification and algal uptake.

Measured and modeled ammonia profiles during fall hypolimnetic anoxia for the 4 years simulated are shown in figure 14, and modeled ammonia through the year near the dam is shown in figure 15 for a representative year (2002). Ammonia was below or close to its analytical detection limit (0.01 mg/L as N) throughout Henry Hagg Lake for most of the year in this study, but measurable concentrations of ammonia were found to accumulate in the hypolimnion at concentrations up to 0.43 mg/L as N once that layer became anoxic in late September. Ammonia can accumulate in the anoxic hypolimnion because no oxygen is present to support nitrification. Sources of ammonia to the hypolimnion include ground-water discharge and the deamination of organic material in the lake sediments. Nitrate can be reduced by bacterial communities to N_2 under anoxic conditions, but further reduction to ammonia is not favored. When the lake turned over in the fall, the accumulated ammonia was mixed and diluted into the larger volume of the reservoir, and the entire reservoir became oxygenated, diminishing the production and stopping the accumulation of ammonia, and increasing the production of nitrate.

While nitrate was included in the Henry Hagg Lake model, no measurements of nitrate concentrations in the lake were available in 2000 through 2002 for calibration, and only a few nitrate samples were collected during the summer of 2003. From these few samples, it appeared that concentrations of nitrate in summer were depleted near the surface and were highest in the hypolimnion. This is consistent with the trend observed by Estrada (2000) in Henry Hagg Lake in 1998–99. That study found the highest concentrations of nitrate in Henry Hagg Lake during winter (0.330 mg/L as N), and depletion in surface waters during the summer (less than 0.016 mg/L as N). Concentrations of nitrate in the hypolimnion remained relatively high (greater than 0.100 mg/L as N) except for the period of hypolimnetic anoxia in the fall. These trends were not always mimicked by the Henry Hagg Lake model, possibly due to inaccurate boundary conditions, inaccurate capture of one or more limnological processes, or both. This is an area where additional data collection, research and additional model refinement may be required for the future. Nitrate is not a critical parameter in characterizing this lake's water quality (recall that blue-green algae can fix atmospheric nitrogen), however, so some error in its representation is acceptable for the purposes of this investigation.

Comparing measured and modeled ammonia profiles at the same location, date, and time produced annual MEs between 0 and 0.01 mg/L as N, MAEs between 0.01 and 0.02 mg/L as N and RMSEs between 0.03 and 0.05 mg/L as N for 2000 through 2003 (table 2). Concentrations of ammonia typically were low (<0.05 mg/L as N), with the exception of samples collected from an anoxic hypolimnion; therefore, it is not surprising that the goodness-of-fit statistics report a relatively small overall error. The model's overall ability to predict the lake's ammonia concentrations, in addition to the correct timing and general magnitude of ammonia accumulation in the lake's hypolimnion, suggests that the most important influences on ammonia were captured by the model with sufficient accuracy.

Algal Biomass and Chlorophyll *a*

Algae tend to grow in lakes in a series of blooms (Horne and Goldman, 1994). Their population is controlled by the availability of light and nutrients, as well as other factors such as settling, zooplankton grazing, and temperature.

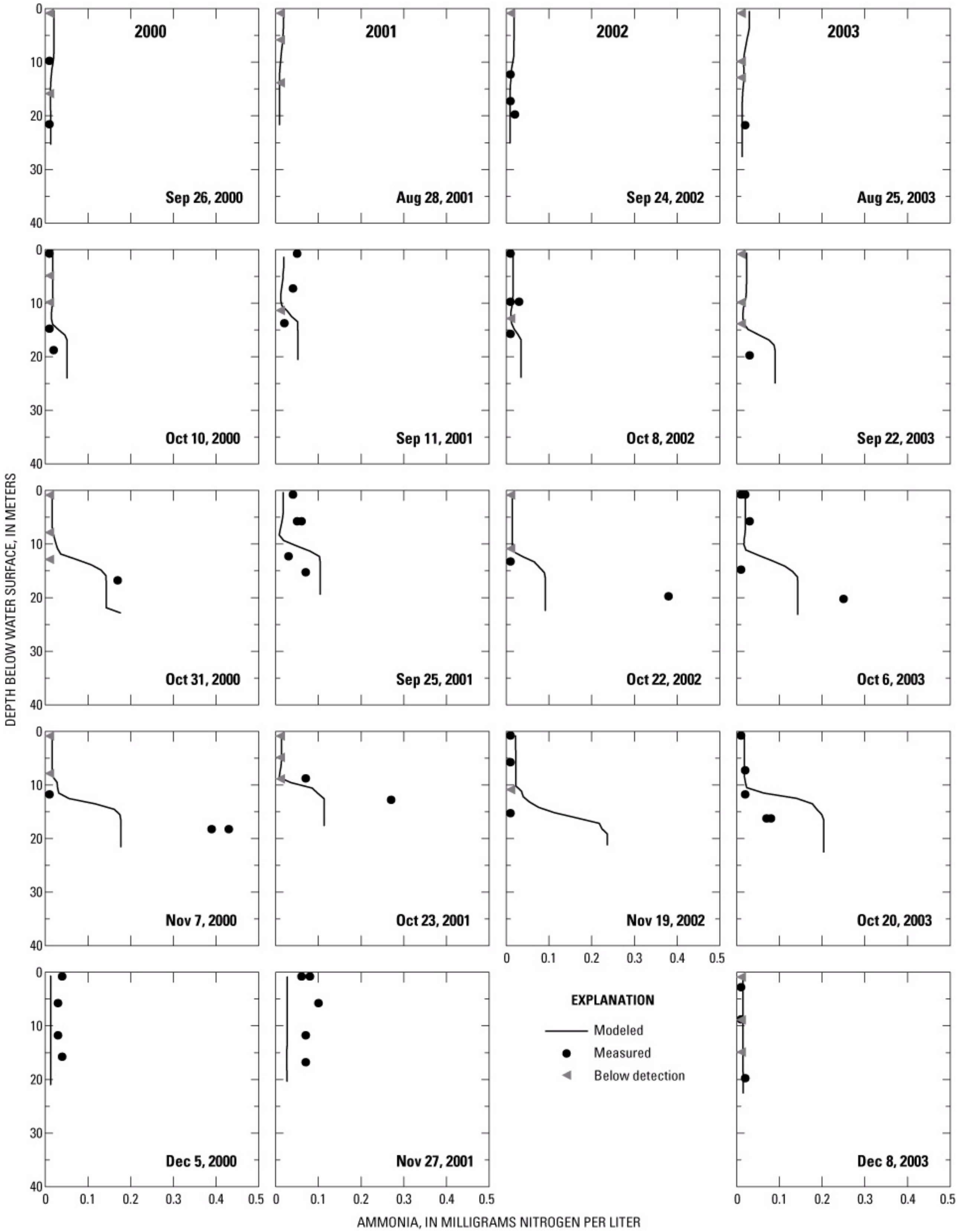

Figure 14. Measured ammonia in the deepest part of the lake near the dam in the fall compared to modeled values from the same location and times for 2000 through 2003. The detection limit for ammonia was 0.01 milligrams per liter as N.

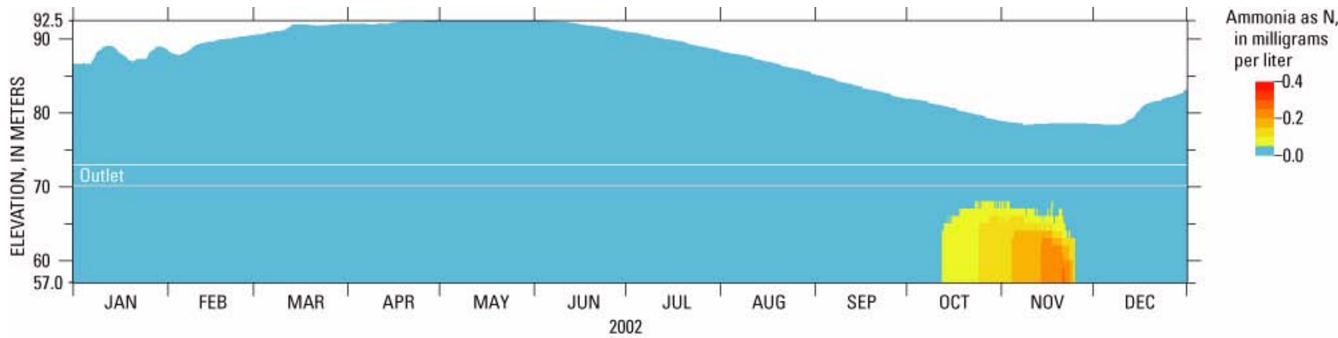

Figure 15. Modeled ammonia concentrations in the deepest part of the lake near the dam in 2002. The elevation range of the lake outlet is noted by the two horizontal lines at elevations of 69.8 and 72.5 meters.

Algae can be a water-quality concern because algal production can result in elevated pH values, and bacterial decomposition of algal cells following bloom crashes can lead to depletion of dissolved oxygen in the water column. Algae also contribute organic carbon to water and contribute to the formation of toxic byproducts in drinking water that form during disinfection. Blue-green algal blooms are of particular concern because they may also produce taste and odor problems in drinking waters, and certain species (e.g. *Anabaena*, *Microcystis*, and others) can produce toxins that are dangerous to humans and aquatic organisms when their concentrations exceed certain thresholds.

Blue-green algae have a number of adaptations that can favor their abundance in reservoirs, allowing them to successfully outcompete other types of algae (Smith, 2001). The ability of blue-green algae to fix nitrogen, for example, allows them to predominate in lakes with low N:P ratios. A stable water column and stable weather conditions also can favor blue-green algal blooms (Sorano, 1997). Gas-filled vacuoles in their cells allow them to rise or sink through the water column to optimize certain growing conditions. They also can grow at higher temperatures that tend to inhibit the growth of other algae.

In this model, algal growth was affected by temperature, light, and the availability of nutrients (nitrogen and phosphorus). The modeled algal growth rate was affected by a combination of ammonia, nitrate, and orthophosphate concentrations. Inorganic carbon and silica concentrations also could be used to help determine the algal growth rate, but these influences were not included in the Henry Hagg Lake model. Algal populations decreased in the model due to respiration, excretion, mortality, zooplankton grazing, and settling to the sediments. When algae died, their biomass became part of the other modeled compartments.

The species composition and dynamics of a lake's algal community can be complex. As such, models of algae necessarily are a gross simplification of what occurs in nature. In Henry Hagg Lake, over 80 different species of algae were identified in the samples taken from 2000 through 2003, and the composition and concentration of algal species in each sampling instance varied greatly (Tualatin River Flow Management Technical Committee, 2000 to 2003). As an example, algal populations in Henry Hagg Lake for 2002 are shown in figure 16, with species grouped together into larger categories such as diatoms or blue-green algae. The model allows the simulation of any number of different algal groups, but each additional group requires separate information on growth rates, mortality rates, and other algal parameters listed in table 3. This information can be difficult to obtain and greatly increases the complexity and uncertainty of the model. An examination of the algal data collected in Henry Hagg Lake, however, showed that at least two algal groups had to be simulated to capture the basic dynamics of the algal community: a blue-green algae group and a general algae group that included all other types, including diatoms, golden-brown algae, and cryptophytes. Model parameters for these two groups are shown in table 3 with their values as used in the calibrated model.

Results comparing modeled and measured total algal biovolume (total of both algal groups) and chlorophyll *a* near the lake surface are shown in figure 17. Algal biomass was simulated by the model; biovolume was calculated directly from biomass using simple density relationships. Surface samples are not always the best indicator of algal activity, but those were the only algae samples taken in the lake. Figure 18 shows modeled chlorophyll *a* at a location near the dam throughout 2002, a representative year. In general, the spring peaks in chlorophyll *a* and algal populations were composed of algae in the model's general algae group. These peaks do not always represent algal growth. For instance, the large spike of algae in February 2000 occurred in coincidence with a large storm. In this case, algae were likely resuspended from lake sediments or washed into Henry Hagg Lake from tributaries (Kurt Carpenter, USGS, oral commun., 2004). The diatom *Melosira italica* is one species commonly found in Henry Hagg Lake during these spring algae peaks. This species has the ability to survive in anoxic sediment for up to 2 years (Horne and Goldman, 1994). Its population appears in the water column in winter and spring and is thought to be due, in part, to scouring from tributary streambeds and resuspension of cells in the lake sediment during storms. The drought year 2001, with no major spring storms, had a very small peak of spring algae, which is consistent with this hypothesized mechanism.

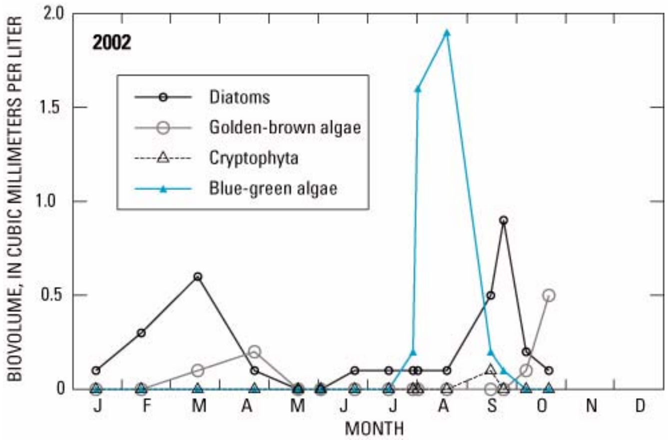

Figure 16. Measured algal biovolume of the four major groups of algae at the surface of Henry Hagg Lake in 2002.

The observed and modeled algal peaks in August-September were mainly due to blue-green algae blooms, the species *Anabaena planctonica* in particular. During these blooms, orthophosphate became depleted in the water column. A lack of orthophosphate is known to control the size of these blooms (Sorano, 1997; Stockner and Shortreed, 1988), and in the model, this directly contributed to the cessation of blue-green algal growth. This suggests that depletion of phosphorus may control the end of the blue-green algae bloom in the lake; however, it is possible that other, unknown factors contribute as well. Elevated water temperature, for example, appeared to be one of the factors that helped to initiate the blue-green algae bloom.

Comparing measured chlorophyll *a* concentrations to modeled values at the same date, time, and location produced annual MEs between -2.3 and -0.3 µg/L, MAEs between 1.9 and 2.4 µg/L and RMSEs between 2.3 and 3.2 µg/L for 2000 through 2003 (table 2). Algae and chlorophyll *a* were only sampled at one depth near the surface of the lake.

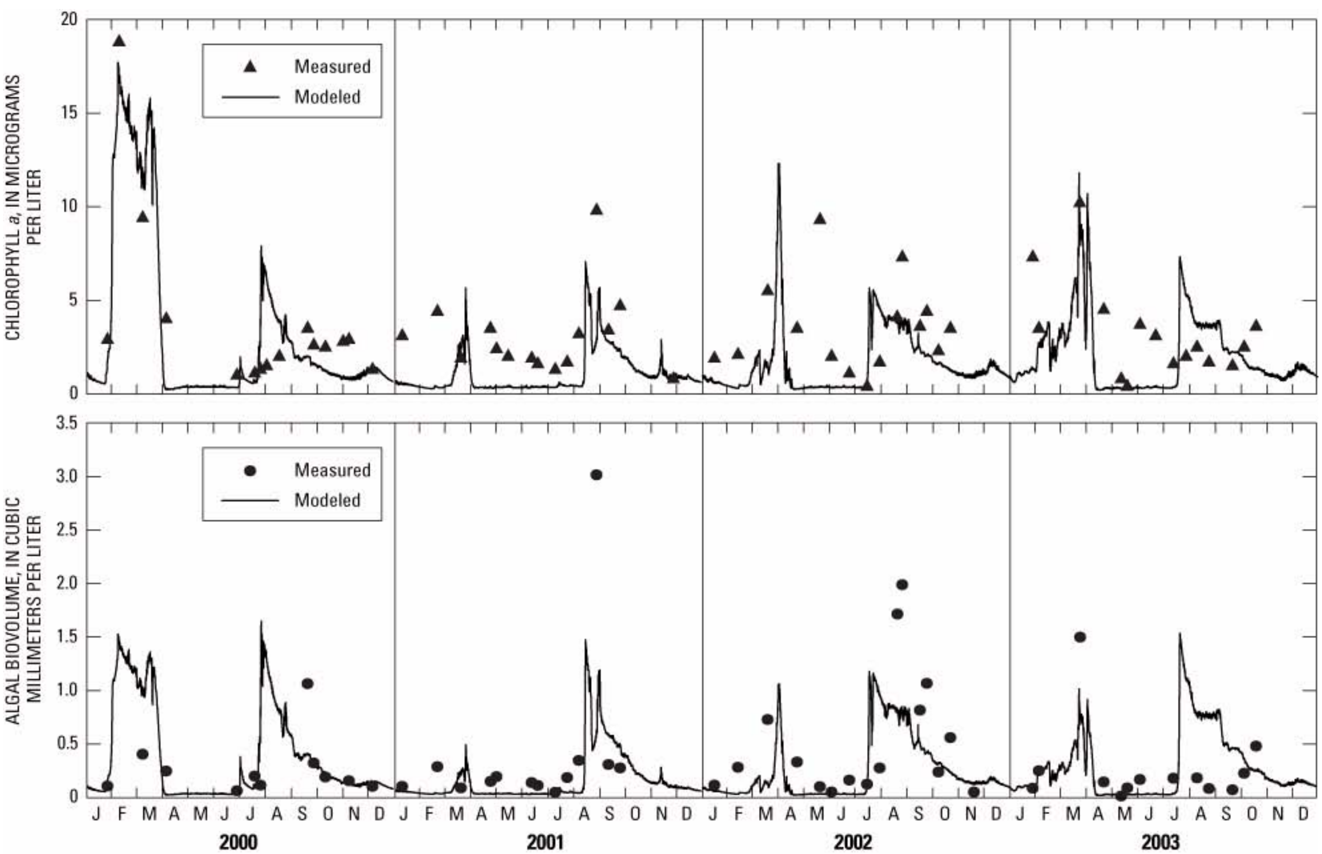

Figure 17. Chlorophyll *a* concentrations near the dam measured at 1 meter depth and algal biovolume measured at the surface compared to modeled values from the same location for 2000–03.

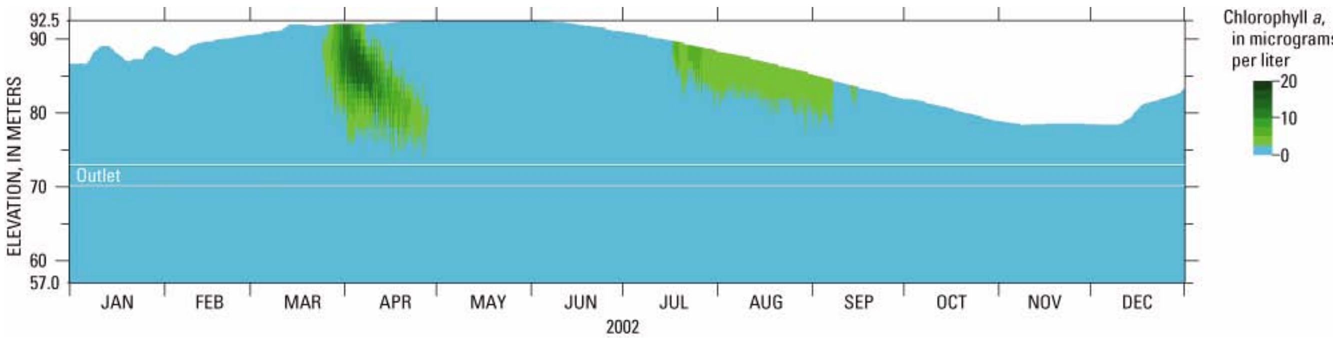

Figure 18. Modeled chlorophyll *a* concentrations in the deepest part of the lake near the dam in 2002. The elevation range of the lake outlet is noted by the two horizontal lines at elevations of 69.8 and 72.5 meters.

However, indirect evidence of algal activity can be seen in the influence of algae on other solutes. For instance, supersaturation of dissolved oxygen sometimes occurred at 5 to 10 m depth, suggesting that algal populations were active there. While the model did not simulate the complex dynamics of all algal species in the lake, it was able to predict the general size and timing of certain algal population changes, including blooms of blue-green algae, which are the algae that most influence Henry Hagg Lake's water quality.

Zooplankton

Zooplankton are an important component of lake food webs, feeding on algae and detrital organic matter, and later providing food for planktivorous fish. Zooplankton are selective in their food choice, and may reject certain algae because of their size or other quality. For example, blue-green algae are less attractive to zooplankton—large blue-green algal colonies can be rejected because of their size, other blue-greens may not be eaten due to a mucilaginous coating. Blue-greens also have very durable cell walls, and some produce toxins (Horne and Goldman, 1994). In addition to their interaction with algae, zooplankton affect lake nutrient cycles through respiration and affect various forms of organic matter through grazing inefficiency and mortality.

One generalized zooplankton group was simulated in the model. Zooplankton grew by feeding on the two algal compartments and the labile particulate organic matter compartment. Each food source was given a preference factor. For instance, zooplankton were assigned a low food preference for blue-green algae. Zooplankton model parameters are listed in table 3, and further details on the implementation of zooplankton in the model are given in Appendix 1.

Measured values for zooplankton are compared to modeled values in figure 19. The modeled values were lower, in general, and far less dynamic than those measured in the lake. In order to simulate higher concentrations of zooplankton in the model without decimating the modeled algal populations, the zooplankton respiration and mortality parameters would have to be set at unreasonably low levels. Measured Henry Hagg Lake zooplankton concentrations in the years of this study ranged from 0.5 to 14 mg/L. Estrada (2000) measured zooplankton in Henry Hagg Lake and found even greater biovolumes, approximately 10 to 10,000 mg/L. It is unknown why these zooplankton concentrations are so varied, but it is possible that populations had a patchy distribution, or that different measurement methodologies led to different measured concentrations. Downstream of Henry Hagg Lake, in the most productive reach of the Tualatin River, zooplankton concentrations were much lower, ranging between 0.001 and 1 mg/L (Rounds et al., 1999).

Compared to other constituents simulated in this study, the model did less well at simulating zooplankton concentrations, and questions remain regarding the zooplankton measurement techniques. It is possible that future zooplankton implementation into the CE-QUAL-W2 code would be more accurate, taking into account different zooplankton groups or age classes (Tom Cole, USACE, oral commun., 2004). Group distinctions would allow the separation of herbivorous zooplankton and carnivorous zooplankton, which are currently combined. However, more groups would require more data to support additional model coefficients and parameters.

Dissolved Oxygen

Factors that affect the concentration of dissolved oxygen in reservoirs include water temperature, inflows and outflows, algal photosynthesis and respiration, zooplankton respiration, ammonia nitrification, decomposition of organic matter in the sediments and water column, and exchange with the atmosphere (Cole and Hannan, 1990). The solubility of oxygen increases with colder water temperatures, while warmer water holds lower amounts of dissolved oxygen. Algal photosynthesis produces dissolved oxygen, while algal respiration consumes oxygen. Conversion of ammonia to nitrate via nitrification requires oxygen. The bacterial decomposition of dead algae and other organic matter in lake sediments can consume substantial amounts of oxygen, which is taken from the overlying water column. The location of the reservoir's outlet structure also can affect the distribution of dissolved oxygen throughout the lake.

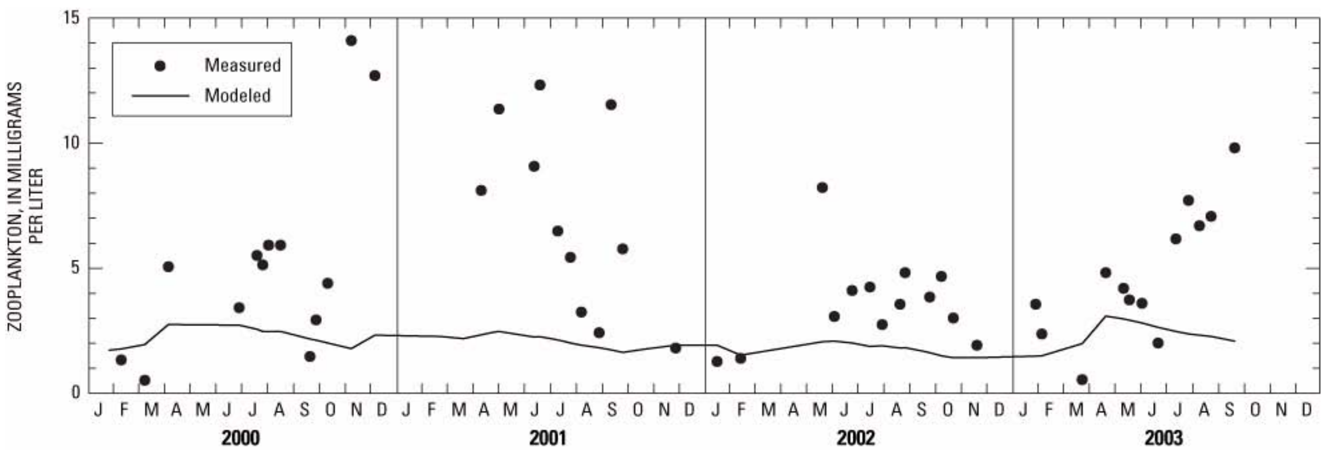

Figure 19. Zooplankton concentrations in Henry Hagg Lake near the dam compared to zooplankton concentrations from the model for 2000–03.

All of these processes are incorporated into the model. The parameters that affect the calibration of dissolved oxygen in the model are listed in table 1. CE-QUAL-W2 allows the user to specify one of many reaeration algorithms; this application used a formulation designed for lakes by Cole and Buchak (1993).

Measured and simulated profiles of dissolved oxygen for 2000 through 2002 are shown in figures 20 through 22. Figure 23 shows modeled dissolved oxygen and temperature concentrations through the length of the reservoir on selected dates in 2000. Figure 24 shows modeled dissolved oxygen at a location near the dam throughout 2002, a representative year. Levels of dissolved oxygen in Henry Hagg Lake were high and homogeneous in winter when the water in the lake was well-mixed and cold. As the lake's surface warmed, oxygen solubility decreased and surface concentrations decreased via losses to the atmosphere. Later, as the hypolimnion became isolated due to lake stratification, the oxygen there was gradually consumed, primarily by sediment oxygen demand. Eventually, the hypolimnion became completely anoxic. This anoxia occurred in late September or early October in most years of this study, but occurred earlier (late August) in the drought year 2001. With colder temperatures and lake overturn in November, dissolved oxygen concentrations in Henry Hagg Lake returned to high levels.

The model can determine dissolved oxygen concentrations of the water withdrawn from the reservoir. This modeled dissolved oxygen concentration in the outflow is compared to measured dissolved oxygen in Scoggins Creek approximately 180 m downstream of the dam in figure 25. The dissolved oxygen concentration in the modeled outflow showed a distinct annual cycle with dissolved oxygen concentrations below 5 mg/L in early fall. Yet the measured concentrations in Scoggins Creek were higher with a less conspicuous seasonal cycle. The difference is due to the fact that the water was aerated between the withdrawal point in the reservoir and the measuring location in the creek downstream. Between those two locations, the water dropped 12 to 27 m in elevation (depending on whether the regular outlet or spillway was in use), and the resulting turbulence at the base of the dam (figure 26) resulted in efficient oxygenation of the outflow water. Saturated values of dissolved oxygen were calculated (U.S. Geological Survey, 1981) from measured water temperature and salinity in the creek and are shown in figure 25. The measured dissolved oxygen in the creek typically was close to saturation and even slightly supersaturated, demonstrating the effectiveness of aeration between the reservoir outlet and the monitor 180 m downstream. The model's ability to predict the dissolved oxygen concentrations at the withdrawal location will be useful in simulating the water-quality effects of potential structural changes to the dam and reservoir, particularly if future withdrawals bypass the aeration basin and are put directly into a pipe.

Comparing measured and modeled dissolved oxygen profiles at the same location, date, and time produced annual MEs between -0.28 and 0.18 mg/L, MAEs between 0.43 and 0.92 mg/L, and RMSEs between 0.60 and 1.24 mg/L for 2000 through 2002 (table 2). The worst fit occurred in 2002, though the fit statistics for that year were still acceptable. That was the year when problems were experienced with the dissolved oxygen probe used for field measurements; it is unclear whether the errors shown in figure 22 were due to measurement error, model error, or both. The overall goodness-of-fit statistics for dissolved oxygen were relatively low (usually <1.0 mg/L), indicating an excellent fit and suggesting that the model was capturing the most important spatial and temporal patterns in the dissolved oxygen data. The model accurately represented the seasonal effects of temperature on oxygen solubility, the importance of sediment oxygen demand, the development and timing of anoxia in the hypolimnion, and the relatively less important effects of algal photosynthesis and respiration. Dissolved oxygen is affected by such a wide range of limnological processes and reactions that it is perhaps the best single gauge of a model's ability to simulate water quality. In this case, the model does an excellent job with dissolved oxygen and, therefore, should be a useful tool for examining and evaluating water quality in Henry Hagg Lake.

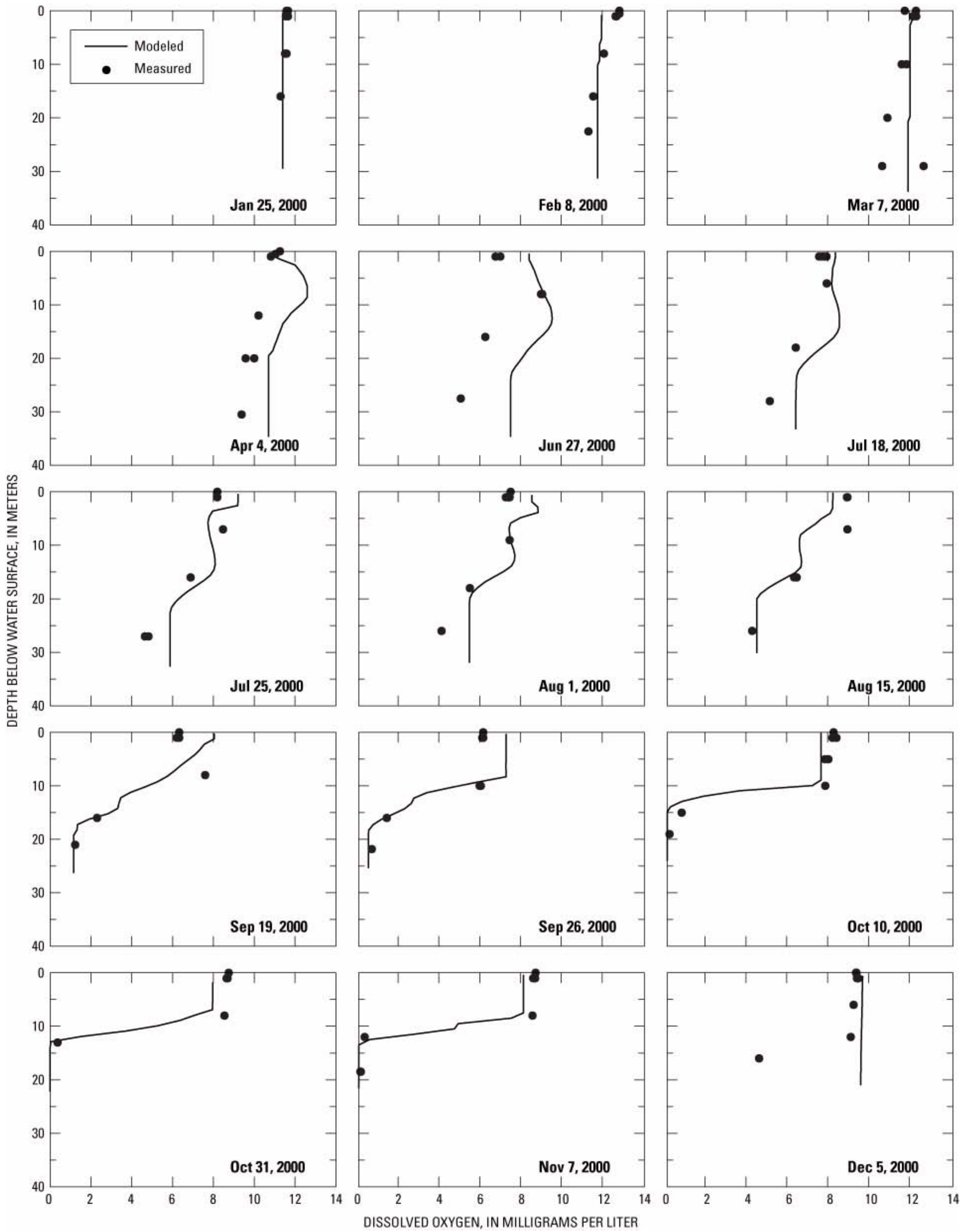

Figure 20. Measured dissolved oxygen profiles in the deepest part of the lake near the dam compared to modeled values from the same location and the same time in 2000.

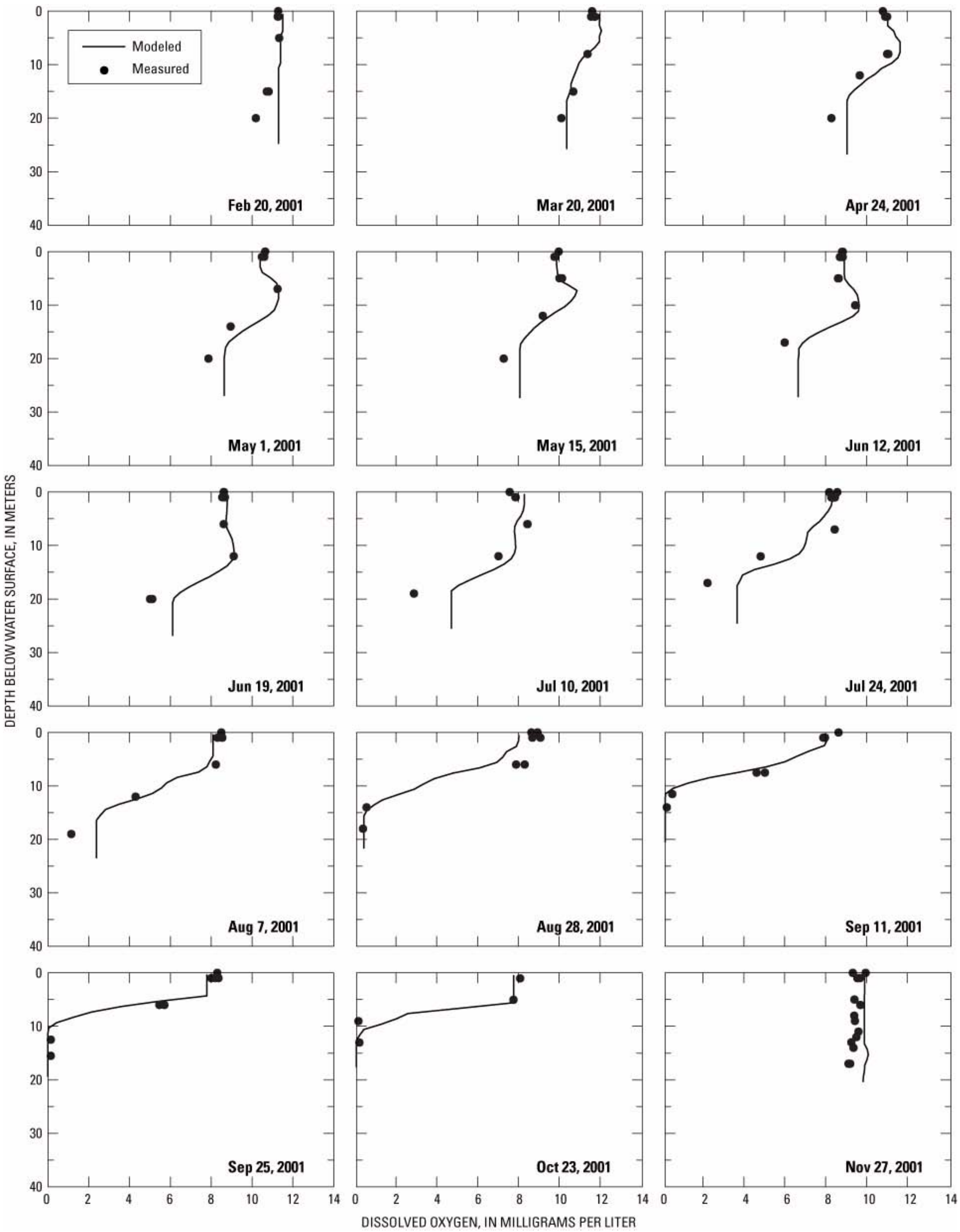

Figure 21. Measured dissolved oxygen profiles in the deepest part of the lake near the dam compared to modeled values from the same location and the same time in 2001.

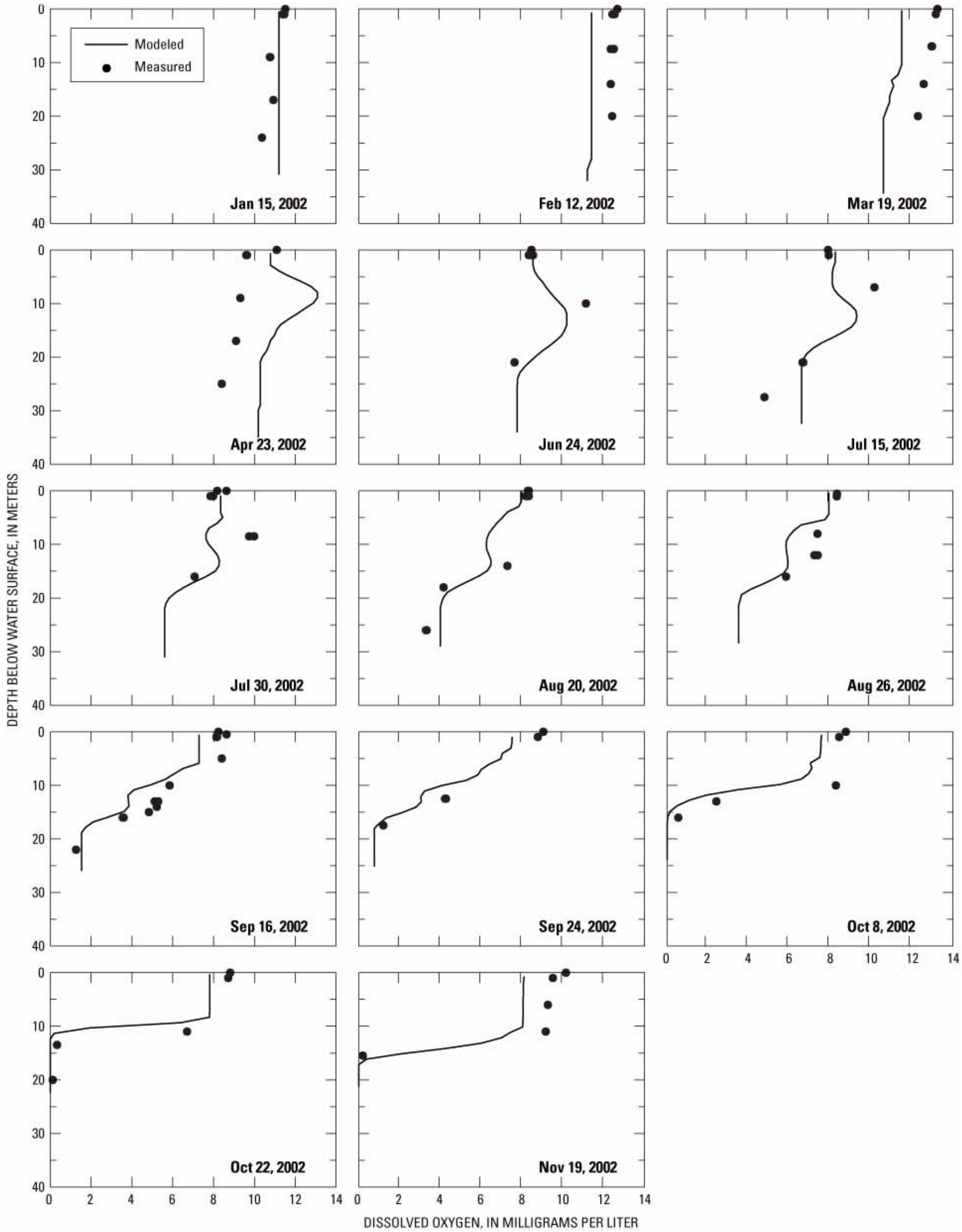

Figure 22. Measured dissolved oxygen profiles in the deepest part of the lake near the dam compared to modeled values from the same location and the same time in 2002.

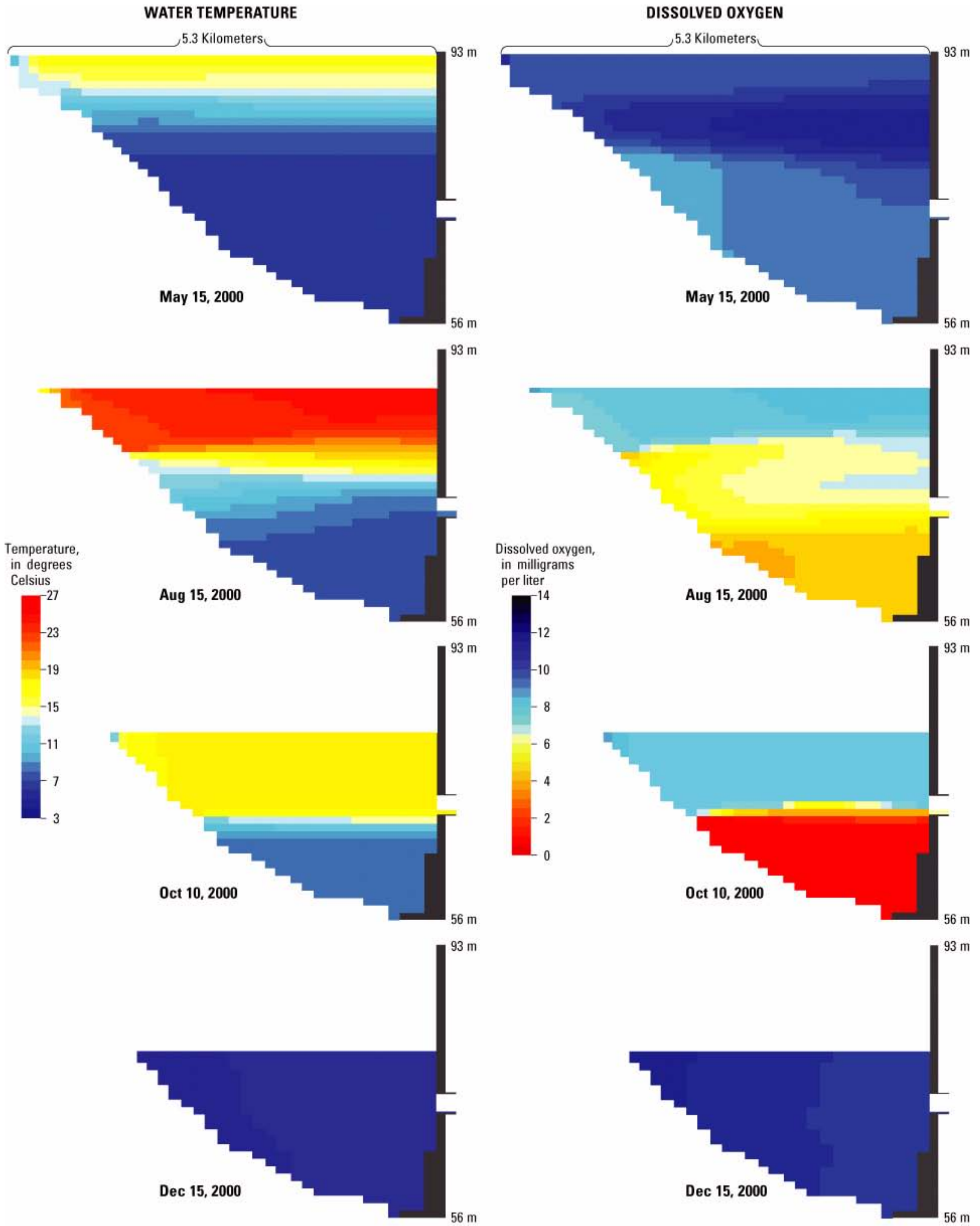

Figure 23. Longitudinal slices through the model grid showing modeled temperature and dissolved oxygen in Henry Hagg Lake on selected dates in 2000, to illustrate the typical seasonal patterns that occur in the lake. Inflows from Scoggins Creek are at the left hand, upstream, end of the figure; Scoggins Dam is at the far right side.

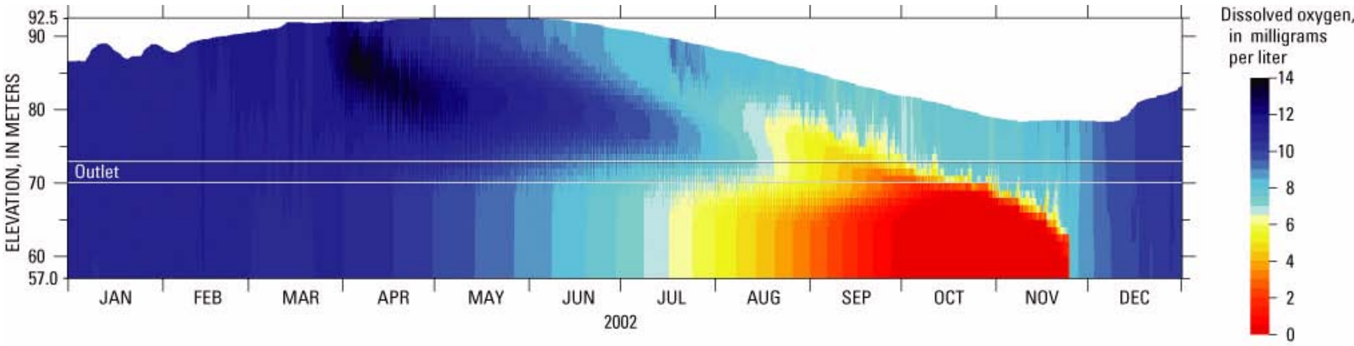

Figure 24. Modeled dissolved oxygen concentrations in Henry Hagg Lake in the deepest part of the lake near the dam in 2002. The elevation range of the lake outlet is noted by the two horizontal lines at elevations of 69.8 and 72.5 meters.

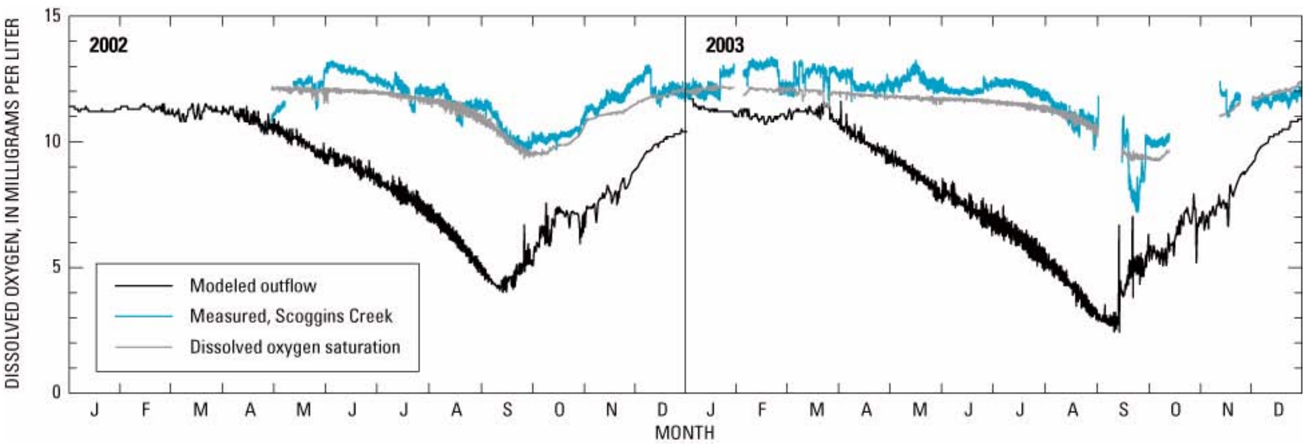

Figure 25. Comparison of modeled dissolved oxygen in the reservoir outflow to measured dissolved oxygen in Scoggins Creek 180 meters downstream of the dam at USGS station 14202980. Calculated values of dissolved oxygen saturation in Scoggins Creek also are plotted, demonstrating that aeration of reservoir outflows was effective.

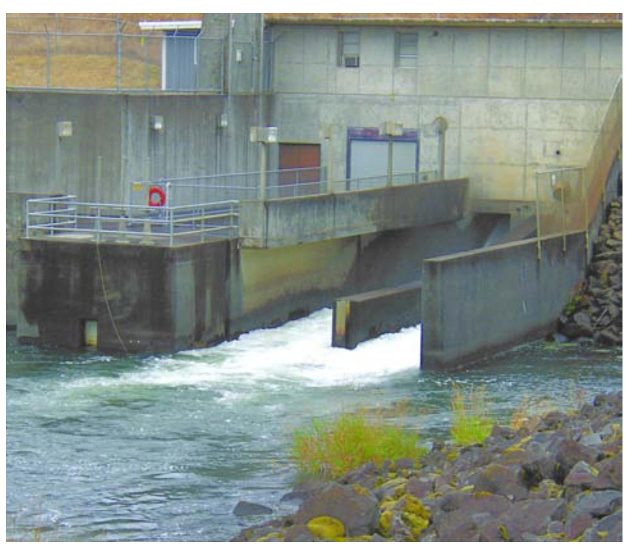

Figure 26. Turbulence at the reservoir outlet entrains a large volume of air, which efficiently aerates the released water as it enters Scoggins Creek. This reaeration process results in dissolved oxygen concentrations near or above saturation.

Sensitivity Analysis

A sensitivity analysis was performed by holding all parameters and inputs constant except the one in question, which was manipulated to examine the model's sensitivity to that variable. The Henry Hagg Lake model has a large number of parameters and inputs, so a complete sensitivity test on each was not feasible. The process of adjusting model parameters during calibration provided a sense of the effect of those parameters on model results. In addition to this, specific sensitivity tests were conducted to examine the effect of varying specific parameters or inputs by 20%. These included the wind sheltering coefficient, inflow phosphorus concentrations, inflow nitrogen concentrations, inflow organic matter concentrations, maximum algal growth rate, zooplankton preference factors for algae, sediment oxygen demand, and the light-extinction coefficient (table 4).

Lake water temperature was sensitive to the elevation of the reservoir outlet, to the temperature of inflows, to meteorologic conditions (such as wind speed), and to the light-extinction coefficient. The wind speed and light-extinction coefficient affected the depth of the thermocline and maximum surface temperatures. A higher wind speed increased surface mixing and evaporative cooling, thus deepening the summer thermocline depth and decreasing summer temperatures at the lake surface. Conversely, a lower wind speed decreased the thermocline depth and increased summer surface temperatures. Lower extinction coefficients deepened the thermocline due to a greater depth penetration of solar energy, while higher values lessened the thermocline depth.

Orthophosphate concentration was sensitive to any change in its major sources or sinks, including algal growth, inflow phosphorus loads, and sediment oxygen demand. Increasing or decreasing the incoming loads of phosphorus or organic matter, which contains phosphorus, directly affected lake phosphorus levels. Factors affecting the growth rate or overall size and distribution of the algal population affected the orthophosphate concentration, demonstrating the close tie between these two constituents. Wind speed, light-extinction coefficients, algal growth rates, and zooplankton preference factors all affected the algae, which in turn had an effect on orthophosphate.

Table 4. Results from sensitivity testing showing percent change in annual, volume-averaged concentrations compared to the base case in 2002.

Parameter	Input (percent change)	Output (percent change)				
		Temperature	Ortho-phosphate	Ammonia	Chlorophyll *a*	Dissolved oxygen
wind sheltering coefficient	-20	-2	-4	0	+13	0
	+20	+2	+9	-2	-12	0
inflow phosphorus	-20	0	-10	-3	-6	0
	+20	0	+10	+2	+6	0
inflow nitrogen	-20	0	0	-3	0	0
	+20	0	0	+2	0	0
inflow organic matter	-20	0	-4	-5	+2	0
	+20	0	+4	+5	-2	0
maximum algal growth rate	-20	0	+12	0	-16	-1
	+20	0	-11	-1	+17	+1
zooplankton preference factors for algae	-20	0	-7	0	+35	+1
	+20	0	+6	0	-20	0
sediment oxygen demand	-20	0	-4	-7	0	+3
	+20	0	+6	+12	0	-3
extinction coefficient	-20	+2	-11	-3	+16	+1
	+20	-1	+9	0	-10	-1

Ammonia concentrations were sensitive to factors directly affecting the release or nitrification of ammonia, including the rate of nitrification and the sediment release rate of ammonia. The latter is specified as a fraction of the sediment oxygen demand rate, so ammonia concentrations also showed sensitivity to sediment oxygen demand. Ammonia concentrations also showed a small sensitivity to changes in the inflow concentrations of nitrogen, organic matter, and phosphorus.

Algal populations were sensitive to many parameters. Factors that affect water temperature, such as those discussed above, could affect the amount and timing of the growth of algal groups that are temperature sensitive, including the blue-green algae. As algal growth was at times phosphorus-limited, changing inflow phosphorus concentrations affected algal populations. Increasing the algal growth rate directly tended to increase the spring bloom, but not the blue-green algae bloom later in the summer, presumably because the larger spring bloom took up the available phosphorus for a longer time period, so that decay processes did not rerelease enough phosphorus to the water column for the summer blue-green algae to use. Algal populations were highly sensitive to changes in their interaction with zooplankton. Increasing the zooplankton preference factors for the two algal groups decreased algal populations throughout the year. Varying inflow nitrogen concentrations by 20% had no effect on algal populations.

The distribution and concentration of dissolved oxygen were controlled by water temperature, sediment oxygen demand, and to a lesser extent by algae. Increasing the sediment oxygen demand rate by 20% caused hypolimnetic anoxia to occur 2 weeks earlier than in the base case. Algae, which produce dissolved oxygen via photosynthesis, also had a small effect on dissolved oxygen. Varying inflow phosphorus, nitrogen, and organic matter concentrations had little effect on dissolved oxygen in the lake.

Summary

The two-dimensional laterally averaged model CE-QUAL-W2 was used to model hydrodynamics, temperature, and water quality in Henry Hagg Lake in northwestern Oregon for the years 2000 through 2003. The model grid accurately replicated the lake's areas and volumes as determined from a 2001 bathymetric survey. Forebay water surface elevation, water temperature, orthophosphate, total phosphorus, ammonia, chlorophyll *a*, algal and zooplankton populations, and dissolved oxygen were calibrated to measured data from 2000 and 2001, then confirmed with data from 2002 and 2003.

The spatial and temporal patterns of water temperature and water quality in Henry Hagg Lake were similar for all years studied. Starting the year well-mixed, cold, and oxygenated, the reservoir developed a thermocline by early summer, isolating cold, dense water below the elevation of the outlet structure. Dissolved oxygen became depleted in the hypolimnion by late August to early October, depending on the year. Accumulation of ammonia began with the onset of hypolimnetic anoxia. Henry Hagg Lake turned over in November, returning to an isothermal, well-oxygenated condition. Algal blooms, including late summer blue-green algae blooms, occurred in all years of this study.

The most important influences on water temperature were meteorological conditions and reservoir operations (stage, withdrawal location). Dissolved oxygen in Henry Hagg Lake was most influenced by water temperature and sediment oxygen demand and, to a lesser degree, periodic algal blooms. The largest bloom of algae typically occurred in August or early September and was dominated by the blue-green alga *Anabaena planctonica*. Model results suggest that this bloom was triggered by late-summer high water temperatures and was limited in size by the availability of phosphorus. Other algal blooms are typically less important to water quality and may be the result of spring storm inflows and resuspension of algal cells.

The calibrated model was capable of simulating the important spatial and temporal dynamics of various constituents in the lake, and successful application of the calibrated model to 2002 and 2003 data confirmed this. Goodness-of-fit statistics for all 4 years varied from acceptable to excellent (mean absolute errors <0.7ºC for temperature and <1 mg/L for dissolved oxygen). Further work is needed to better simulate some of the complexities of the algae and zooplankton populations.

This calibrated model will next be used to simulate the effects of structural changes to Scoggins Dam that are under consideration. Proposed options include raising the dam height by 6.1 or 12.2 m (20 or 40 ft), installing a water pipeline directly from the lake to a major user, installing different or additional withdrawal structures, including the possibility of a selective withdrawal tower, and routing water from the upper Tualatin River across a watershed divide and into Henry Hagg Lake via Sain Creek. The model will help predict water temperature and water-quality effects from such management actions.

Acknowledgments

This study was done with cooperative funding provided by Clean Water Services and the USGS. We thank Chuck Kingston (JWC), Art Woll (JWC) and everyone associated with the Henry Hagg Lake monitoring program for collecting the temperature and water-quality samples that allowed for model calibration. Sample results and other data used for modeling were provided by Bernadine Bonn (CWS), Jan Miller (CWS), Wally Otto (TVID), and Bob Wood of the District 18 Watermaster's Office. The Bureau of Reclamation provided a GIS dataset of Henry Hagg Lake bathymetry, and Steve Sobieszczyk (USGS) assisted with GIS portions of this project. Discussions with Kurt Carpenter (USGS), Dennis Lynch (USGS) and Tom Vander-Plaat (CWS) were helpful in model development and calibration. Thanks to Reed Green (USGS), Chris Berger (Portland State University) and Kurt Carpenter (USGS) for their reviews of this document.

References Cited

American Public Health Association, 1998, Standard Methods for the Examination of Water and Wastewater, 20th edition: Water Environment Federation, 1220 p.

Bowie, G.L., Mills, W.B., Porcella, D.B., Campbell, C.L., Pagenkopf, J.R., Rupp, G.L., Johnson, K.M., Chan, P.W.H., Gherini, S.A., and Chamberlin, C.E., 1985, Rates, constants, and kinetics formulations in surface water-quality modeling, Second edition: U.S. Environmental Protection Agency EPA/600/3-85/040 [variously paged].

Bureau of Reclamation, 2001, Tualatin Project Henry Hagg Lake Oregon—Area and capacity tables: Bureau of Reclamation, 83 p.

Cole, T.M., and Buchak, E., 1993, CE-QUAL-W2: A two-dimensional, laterally averaged, hydrodynamic and water-quality model, version 2.0: U.S. Army Corps of Engineers [variously paged].

Cole, T.M. and Hannan, H.H., 1990, Dissolved oxygen dynamics. in Thornton, K.W., Kimmel, B.L., and Payne, F., Reservoir Limnology: Ecological Perspectives. John Wiley and Sons, Inc. Chapter 4, 71–107.

Cole, T.M., and Wells, S.A., 2002, CE-QUAL-W2: A two-dimensional, laterally averaged, hydrodynamic and water-quality model, version 3.1: U.S. Army Corps of Engineers, Instruction Report EL-02-1 [variously paged].

Estrada, M.A., 2000, The dynamics of the planktonic community of two Oregon reservoirs: Portland State University M.S. Thesis, 199 p.

Ferrari, R.L., 2001, Henry Hagg Lake 2001 Survey: Bureau of Reclamation, 17 p.

Horne, A.J., and Goldman, C.R., 1994, Limnology, Second Edition: McGraw-Hill, Inc., New York, 576 p.

Knutson, M.T., 1993, Modeling of flow and water quality in Henry Hagg Lake near Forest Grove, Oregon. M.S. Thesis, Portland State University, 146 p.

Montgomery Watson Harza, 2004, Tualatin Basin water supply feasibility study—Final report: Available upon request from Clean Water Services, Hillsboro, Oregon, 79 p.

Rounds, S.A., Wood, T.M., Lynch, D.D., 1999, Modeling discharge, temperature, and water quality in the Tualatin River, Oregon: U.S. Geological Survey Water-Supply Paper 2465–B, 121 p.

Schlicker, H.G., and Deacon, R.J., 1967, Engineering geology of the Tualatin Valley region, Oregon: Oregon Department of Geology and Mineral Industries Bulletin 60, 103 p.

Smith, V.H., 2001, Blue-green algae in eutrophic fresh water: Lakeline, spring, p. 34–37.

Sorano, P.A., 1997, Factors affecting the timing of surface scums and epilimnetic blooms of blue-green algae in a eutrophic lake: Canadian Journal of Fisheries and Aquatic Sciences, v. 54, p. 1965–1975.

Stockner, J.G., and Shortreed, K.S., 1988, Response of *Anabaena* and *Synechococcus* to manipulation of nitrogen:phosphorus ratios in a lake fertilization experiment: Limnology and Oceanography, v.33(6, part 1), 1348–1361.

Taylor, G.H., 2002, The climate of Oregon, climate zone 2, the Willamette Valley, Oregon Climate Service: Special Report 914, accessed July 7, 2004, at http://www.ocs.orst.edu/pub_ftp/reports/zone/zone2.html.

Tualatin River Flow Management Technical Committee, 2000, 2000 Annual report, accessed November 8, 2004, at http://www.co.washington.or.us/deptmts/wtr_mstr/downloads/FlowRpt_2000.pdf.

Tualatin River Flow Management Technical Committee, 2001, 2001 Annual report, accessed November 8, 2004, at http://www.co.washington.or.us/deptmts/wtr_mstr/downloads/FlowReport.2001.pdf.

Tualatin River Flow Management Technical Committee, 2002, 2002 Annual report, accessed November 8, 2004, at http://www.co.washington.or.us/deptmts/wtr_mstr/downloads/FlowRpt2002.pdf.

Tualatin River Flow Management Technical Committee, 2003 Annual report: Available upon request from Clean Water Services, Hillsboro, Oregon, 50 p.

U.S. Environmental Protection Agency, 1983, Methods for chemical analysis of water and wastes: EPA-600/4-79-020, 552 p.

U.S. Environmental Protection Agency, 1993, Methods for the determination of inorganic substances in environmental samples: EPA/600/R-93/100, 79 p.

U.S. Geological Survey, 1981, New tables of dissolved oxygen saturation values: Quality of Water Branch Technical Memorandum 81.11, accessed July 15, 2004, at http://www.water.usgs.gov/admin/memo/QW/qw81.11.html.

Glossary

Adsorption Adherence of ions or molecules in solution to the surface of a solid.

Anoxia The absence of dissolved oxygen.

Coprecipitation The incorporation of elements into other compounds as they precipitate as solids from solution.

Deamination Process in which the breakdown of amino acids in organic matter generates ammonia.

Denitrification The conversion of nitrogen oxides, such as nitrate and nitrite, to molecular nitrogen or other nitrogen oxides.

Epilimnion The upper, warmer and less dense layer of a thermally-stratified lake.

Hypolimnion The cool, dense lower layer of water in a thermally stratified lake.

Nitrification The oxidation of ammonia and ammonium sequentially to nitrite and then nitrate.

Nutrient Elements or compounds essential for growth and development of organisms, including carbon, nitrogen and phosphorus species.

Oligotrophic Waters that are nutrient-poor with low primary productivity.

Orthophosphate Inorganic phosphorus dissolved in water (PO_4^{3-}).

Photic Zone The upper layer of water down to the depth of effective light penetration, where primary production occurs.

Sediment Oxygen Demand The rate of dissolved oxygen consumption at the sediment/water interface.

Stratification The arrangement of a waterbody into two or more layers with differing characteristics, such as temperature and density.

Thermocline The region of a thermally stratified lake in which there is a rapid change in temperature with water depth.

Total Kjeldahl Nitrogen (TKN) The concentration of nitrogen present as ammonia or bound in organic compounds.

This page left intentionally blank

Appendix 1

This page left intentionally blank

Appendix 1.

The zooplankton code added to CE-QUAL-W2 for the Hagg Lake application was modified from CE-QUAL-R1, the one-dimensional USACE lake water-quality model and is largely identical to that documented by Rounds et al. (1999) in their Tualatin River CE-QUAL-W2 model. In this formulation, only one zooplankton group was simulated. Most zooplankton processes were controlled by temperature rate modifiers. The zooplankton population was initialized at the start of a simulation, and grew by grazing on algae and labile particulate organic matter (fig. A-1). Grazing was not completely efficient, and a parameter between 0 and 1 determined what proportion of food was actually consumed and assimilated. Egested food was routed to the labile particulate organic matter compartment. Because CE-QUAL-W2 could simulate more than one algal group, the zooplankton formulation allowed separate zooplankton food preference factors, between 0 and 1 for each algae group, and for labile particulate organic matter (LPOM). A factor of 1 corresponded to food that was desirable, and a factor of 0 corresponded to food that was never eaten. When food concentrations were below a specified threshold level, zooplankton grazing halted. A Michaelis-Menton formulation with a half-saturation food concentration produced grazing rates proportional to food concentration at low food concentration, but which leveled off at higher concentrations of food.

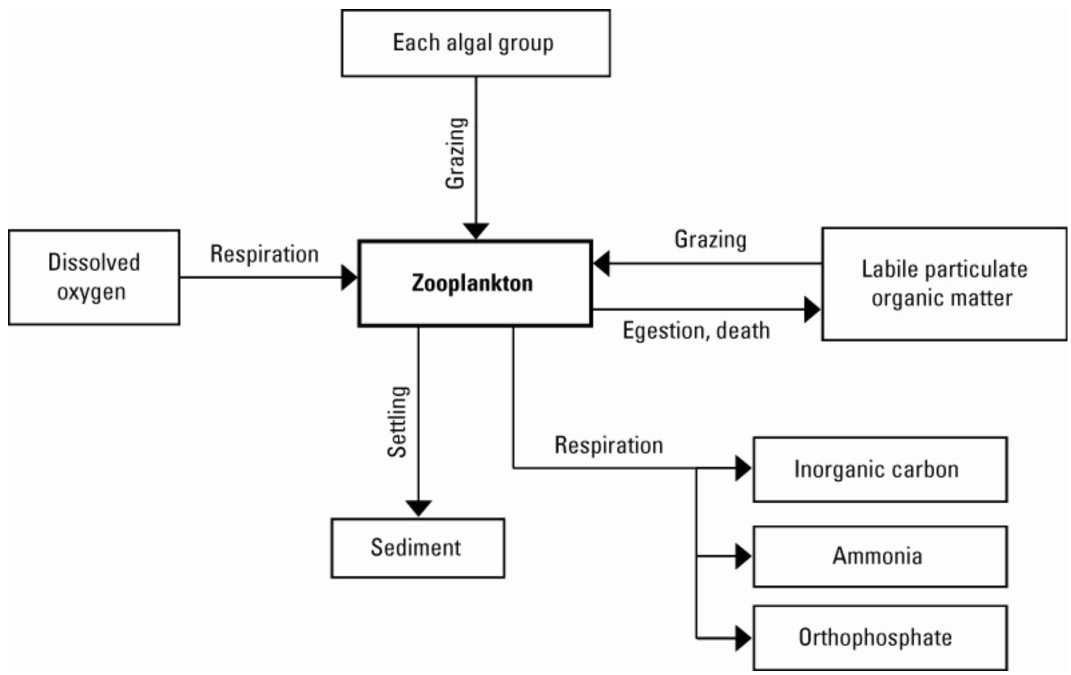

Figure A-1. Schematic diagram of the model compartments affected by zooplankton and the processes through which they are connected.

Zooplankton respiration released ammonia, orthophosphate, and inorganic carbon to the water. Respiration also consumed dissolved oxygen. Zooplankton concentrations were decreased via mortality, which increased the concentration of the labile particulate organic matter compartment. Zooplankton concentrations always remained above a minimum threshold level; at the threshold level, respiration and mortality were set to 0. At dissolved oxygen concentrations less than 2 mg/L, grazing ceased and mortality rates doubled. Finally, zooplankton were allowed to settle or be buoyant through the assignment of a positive or negative settling velocity, respectively, and zooplankton contribute to light extinction in the same way as particulate organic matter.

Equations showing the source/sink flux rates for the zooplankton interactions are documented below. The equations are similar to those documented by Rounds et al. (1999) and are presented in a format similar to that used by the CE-QUAL-W2 user manual (Cole and Wells, 2002).

$$S_z = (K_{zg}\lambda_{zg}\gamma_{zr}\gamma_{zf}e_{zg} - K_{zm}(1-\gamma_{zf}) - K_{zr}\gamma_{zr})\Phi_z - \omega_z\frac{\partial\Phi_z}{\partial z}$$

Where

S_z = source/sink flux rate for zooplankton, g/m^3/s;
z = cell height, m;
Φ_z = zooplankton concentration, g/m^3;
ω_z = zooplankton settling rate, m/s;
K_{zg} = zooplankton maximum grazing rate, 1/s;
K_{zm} = zooplankton maximum mortality rate, 1/s;
K_{zr} = zooplankton maximum respiration rate, 1/s;
γ_{zr} = zooplankton temperature rate multiplier, rising limb;
γ_{zf} = zooplankton temperature rate multiplier, falling limb;
e_{zg} = efficiency of zooplankton grazing, fraction between 0 and 1;
λ_{zg} = zooplankton food availability factor.

$$\lambda_{zg} = \frac{p_{lpom}\Phi_{lpom} - \mu_z + \sum_i p_{a_i}\Phi_{a_i}}{h_{zg} + p_{lpom}\Phi_{lpom} + \sum_i p_{a_i}\Phi_{a_i}}$$

Where

Φ_{lpom} = concentration of labile particulate organic matter, g/m^3;
Φ_{a_i} = concentration of algal group i, g/m^3;
p_{lpom} = zooplankton grazing preference factor for LPOM, fraction between 0 and 1;
p_{a_i} = zooplankton grazing preference for algal group i, between 0 and 1;
μ_z = threshold food concentration, below which no grazing occurs, g/m^3;
h_{zg} = half-saturation food concentration for zooplankton grazing, g/m^3.

Back Cover:

Top:

The western portion of Henry Hagg Lake, showing the pier near picnic area C, taken on Sept. 22, 2004.

Bottom:

Henry Hagg Lake, looking down the Sain Creek arm, taken on Sept. 22, 2004.

Both photographs by Stewart Rounds (U.S. Geological Survey).

USGS

Sullivan and Rounds—Modeling Hydrodynamics, Temperature, and Water Quality in Henry Hagg Lake, Oregon, 2000–03—SIR 2004-5261

125 years of science for America